Response to Editors comments:

Non-public comments to the Author:
1. P1 L20: No need for "human induced"; "fossil fuel emissions" already indicates its relationship to humans

Response: This has been taken care of (L20, L41; where L is line in revised manuscript).

2. P1 L22-26: sentence structure is awkward; please use semi-colons instead of full stops; the first word in each sub-phrase should be in lowercase; insert "and" between the second and third sub-phrases

Response: This has been taken care of (L22-L27).

3. Balance the Abstract with respect to the importance of EVI, NDVI, and RDVI in the analysis; you do not mention EVI

Response: We have now incorporated which vegetation indices that were used in the analysis (L25-L27).

4. P2 L42: "are even the main biome…"; in context of the entire sentence, I am unsure what this means; please rephrase

Response: This has been changed to: "Mean carbon dioxide (CO_2) uptake by terrestrial ecosystems is dominated by highly productive lands, mainly tropical forests, whereas semi-arid regions are the main biome driving its inter-annual variability (Ahlström et al., 2015; Poulter et al., 2014). Semi-arid regions even contribute to 60% of the long term trend in the global terrestrial C sink (Ahlström et al., 2015)." (L41-44)

5. P2 L49: is "productivity" the right word? Do you mean "production"? Please make changes throughout the manuscript.

Response: This has been taken care of throughout the manuscript.

6. P2 L50: "under high pressure" is ambiguous; you may rewrite as "under threat"

Response: This has been taken care of (L51).

7. P2 L59: "Climate is thus another factor…to their vulnerability to moisture conditions"; this sentence could be made into two separate sentences. Remove the "and" and capitalize the "S" in "semi-arid region such as…"

Response: This has been taken care of (L57-58).

8. Many unnecessary uses of "the"; you may remove without loss of meaning

Response: This has been taken care of throughout the manuscript.

9. P2 L63: "defined as the efficiency to convert absorbed solar light into CO2 uptake…" can be written as "defined as the conversion efficiency of absorbed sunlight to C uptake…"

Response: This has been taken care of (L62).

10. P2 L74: "level" is not needed

Response: This has been taken care of (L73).

11. P3 L75-80 (and other places in the manuscript): Do not change verb tense midsentence

Response: This has been taken care of throughout the manuscript.

12. P3 L103-105: "To evaluate…"; awkward sentence, please rephrase; what is there to evaluate?

Response: This has been changed to: "To investigate if the recently released MOD17A2H GPP (collection 6) product is better at capturing GPP for the Sahel than collection 5.1." (L102-105)

13. P4 L136 (and other places in the manuscript): "according" should be "according to"

Response: This has been taken care of throughout the manuscript.

14. P5 L156 and P7 L236-237: these sentences are not needed; just indicate what was used/done, not what was needed; similar filler is used throughout the manuscript

Response: Fillers have been removed throughout the manuscript.

15. Never start a sentence with a symbol, a number, or an acronym. Please spell out each time when used at the start of a sentence; make changes throughout the manuscript.

Response: This has been taken care of throughout the manuscript.

16. Simplify hydrological and meteorological to "hydrometeorological"

Response: This has been taken care of throughout the manuscript.

17. P5 L173: "the fitting was insignificant (p-value < 0.05)…"; should it read "p-value > 0.05"?

Response: This has been taken care of (L167).

18. P5 L175: can be modified as "using a 30-day moving window with a 1-day time step"; not clear; please elaborate

Response: This has been taken care of (L168).

19. The manuscript needs some level of streamlining; e.g., results appearing in the Methods section (e.g., P6 L213-214) should be moved to their appropriate section; redundant material throughout the manuscript should be removed (e.g., P8 L274, P10 L357-359, and other places in the manuscript)

Response: The result in the method section in the previous version of the manuscript has been moved to the supplementary material. Redundant material throughout the manuscript has been removed.

20. P5 214-216: I am unsure what you mean by this statement

Response: This section has been completely changed (L206-L214).

21. Many statements in the manuscript are vague in nature, please be more specific (see e.g., P5 L178 and L214-215, and P10 L355 with "…to a certain level…")

Response: We have tried to be more specific throughout the revised manuscript.

22. P7 L247: I am unsure what is meant by "robustness"; please be specific

Response: This has been revised throughout the manuscript.

23. P8 L253-270: simplify detail; you may consider placing intermediate equations in a Table

Response: We fully agree, we have simplified this section and removed some of the unnecessary intermediate equations (Section 2.4.2).

24. P8 L273: "We used 200 iterations and different measurements sites…"; this suggests that 200 different measurement sites were used; I know this is not the case, please rephrase if the sentence is needed; i.e., "different" is vague, be specific

Response: This has been clarified in the revised manuscript (L258-260).

25. P8 L280: "left-out subsamples"; this was not addressed before, please introduce in the appropriate place

Response: Within the bootstrap simulation methodology some sites were included and some were left-out. This has been clarified in the revised manuscript (L258-260).

26. P8 L282 (and other places in the manuscript): "in situ variables" is better termed as "independent variables"; the emphasis is on the fact that the variables are independent predictors of a dependent variables opposed to the variables being measured in the field

Response: This has been changed throughout the manuscript.

27. A flowchart of methods and information flow would be helpful in understanding the work

Response: It is our hope that the revised clarified manuscript makes this flowchart unnecessary. However, if this is still considered required after the review of the revised manuscript we are naturally willing to include such a flowchart.

28. P10 L335: "works on average well…" should be "works well on average…"; similar constructions can be found throughout the manuscript, please consider changing

Response: This has been taken care of throughout the manuscript.

29. P11 L366-367: "…including blue-band information…"; what is the significance of this? Also, the entire sentence (L366-368) needs revising, currently awkward

Response: We agree, this sentence has been removed.

30. I am pleased to see that you have considered to incorporate additional maps showing regional impact on GPP and other variables; this added information should help you develop a more convincing Discussion; redundancy in the current discussion should be removed

Response: Redundancy in the previous discussion has been removed and the additional maps are discussed in the revised manuscript.

31. The heading of Table 3 is awkward, "statistics" do not "study"; please revise

Response: This has been taken care of (Table 3).

Response to comments by Reviewer #1

A. Summary
This paper uses data from six eddy covariance flux sites distributed across the Sahel of West Africa to examine patterns in space and time of carbon fluxes (GPP) as characterized by two key canopy-scale parameters (maximum photosynthetic uptake, called Fopt in this paper, and initial quantum yield, termed alpha). The authors also explore the relationships between the two GPP parameters and a variety of satellite vegetation indices providing (in theory at least) opportunities for spatial upscaling of the site-based results. This is an interesting paper reporting useful results.

Response: Thank you very much, and also thank you for insightful comments that helped improving the manuscript.

B. Main Points
1. Regional GPP estimation. It is a pity the authors didn't take the final step to evaluate GPP across the region using the fitted models. At least, we don't see a map of these estimates, only point-based comparisons with the 6 field sites. In Section 2.4.1 the authors describe a "full model" for the regression tree used to characterize fluxes and predict Fopt and alpha at the field sites. In Section 2.4.2 they continue to describe an approach to derive parameters on a pixel-by-pixel basis where not all edaphic data (e.g. soil moisture) are available. However, we don't see the results of this analysis in the form of a map or other representation. Could this be added?

Response: We agree with the reviewer; in the previous version of the manuscript we did not include the full gridded map because the spatial up-scaling requires some very heavy computer processing. However, we have now borrowed computer power from the university, and in the revised version of the manuscript we have included a full gridded map of peak F_{opt}, peak α and an annual sum of GPP (L322-L326; where L is line in revised manuscript , Fig. 5).

2. Prior work: The authors should refer to some considerable prior work that will be relevant to this analysis. See Global Change Biology 4, 523-538 (1998) and numerous HAPEX-Sahel papers in the J. Hydrology 1997 for earlier and quite detailed analysis of flux measurements in Sahelian vegetation. The GCB paper, for example, analyses Fopt and alpha as a leaf-level variable in considerable detail. Note that the canopy scale Fopt and alpha investigated here incorporate the effects of changing LAI during the season. This rather complicates the situation for this analysis, as the authors state on line 351.

Response: Thank you for this suggestion, we agree that it was a good idea to extend the comparison of the results of our analysis to the results of previously published research. This has been incorporated into the revised manuscript (L360-374).

3. Peak uptake rates: the field measurements at some sites seem abnormally high. The earlier data in the GCB paper references above was for a southern Sahel site with LAI likely higher than any of these sites, but with maximum Fopt of only -15-20 umol m-2 s-1.

Response: 1) The leaf area index value of the HAPEX–Sahel West-Central fallow savanna site in (Hanan et al., 1998) is not larger than at the Dahra and Kelma sites, which are the two sites of our study with very high F_{opt} and α. Peak LAI is 2.1 for Dahra and 2.7 for Kelma, so it is considerably higher than 1.2 as given in (Hanan et al., 1998). The higher LAI can thereby explain parts of the higher F_{opt} estimates.
2) (Hiernaux et al., 2009) and (Dardel et al., 2014) showed above ground peak biomass in southwestern Niger which are comparable, and nowadays slightly lower than what is reported for the Gourma area (which in addition receives less rain).

Hanan et al 1997 (J Hydrology) report above ground peak biomass of 1000 and 1500 kg/ha for the grass and shrub fallow sites, which is much lower than what is reported for the Dahra site (Mbow et al., 2013), which also receives less rainfall. This is in line with a productivity gradient over these 3 sites, possibly caused by soil fertility and fallow management in southwestern Niger.
3) The reason for high estimates of F_{opt} and α are the very high net CO2 fluxes measured by the eddy covariance systems. For the Dahra field site, we have performed a rigorous quality check of the data, please see (Tagesson et al., 2016) and we are certain that the measured values are correctly measured. Tagesson et al. (2016) have tried to explain the high net CO_2 flux values by that there is a combination of dense herbaceous C4 ground vegetation, high soil nutrient availability, a grazing pressure resulting in compensatory growth and fertilization effects, and the West African Monsoon bring a humid layer of surface air from the Atlantic, possibly increasing vegetation productivity for the most western part of Sahel. This info has been included in the revised manuscript (L360-374).

4. Possible unit issues: this is an impertinent question, but looking at the massive multipliers between the author's estimates and independent estimates in Figures 2 (incoming PAR) and 3 (GPP) I couldn't help wondering if there might be some unit issues. In the case of PAR the conversion of PAR in W/m2 to umol m-2 s-1 varies somewhat based on solar angle and atmospheric conditions but is typically 4.2 umol/W. This is more than the 3.09 of the fitted slope, but is it really possible that the ERA PAR product is underestimating actual incoming PAR so consistently by a whopping 70% ! Similarly for Figure 3, if the MODIS product is in units of g/m2/day carbon and the authors have retained their data in units g/m2/day CO2 this would give an inherent slope in Figure 3 of 12/44 = 0.273. Again this doesn't entirely account for their calculated slope of 0.17, but might be worth double-checking.

Response: Yes, we absolutely understand your concern here, and we have been looking at these conversions many times to make absolutely sure that the conversions are correctly done:

1. **PAR values:**

The average raw in-situ PAR = 483 µmol m-2 s-1

The average raw ECMWF PAR = 350503 (J m-2 summed for 3 hours)

To get ECMWF PAR to (W m-2): raw ECMWF PAR was divided by (60sec*60 minutes*3 hours) =>
Average ECMWF PAR (W m-2) =350503/(60*60*3)= 32 W m-2.

To convert ECMWF PAR (W m-2) to µmol m-2 we multiplied with 4.57 (Sager and McFarlane, 1997):

Average ECMWF PAR (µmol m-2 s-1) =32*4.57= 148 µmol m-2 s-1

Average in-situ PAR (µmol m-2 s-1)/ Average ECMWF PAR (µmol m-2 s-1) = 483/148 = 3.2

So we think that the PAR conversion is correctly done. We recently found out that the issue is related to a major error in the code of ECMWF surface PAR:
"The surface incident value (code 58) seems erroneously low. For example, in locations in the Celtic Sea, surface PAR is typically around 20% to 25% of the clear sky value (code 20), and about a third of in-situ measurement of surface PAR. Cause: We have shortwave bands that include 0.442-0.625 micron, 0.625-0.778 micron and 0.778-1.24 micron. PAR is coded as if it was intending to sum all of the radiation in the first of these and 0.42 of the second (to

account for the fact that PAR is normally defined to stop at 0.7 microns. However, PAR is in fact calculated from the sum of the second band plus 0.42 of the third." (ECMWF, 2016).
This indicates that the ERA-interim surface PAR product is actually not PAR, but rather incoming red and near infrared. However, we still intend to use this data source since we relate the gridded ECMWF PAR to in-situ measured PAR and used this relationship to convert ECMWF PAR to the proper level. The relationship should be ok, even if it is relating in-situ PAR to a different part of the spectrum; the final product is still PAR at a reasonable level. The conversion of ERA interrim PAR is described in the revised manuscript (L207-214).

2. **MODIS GPP:**

An example for GPP of Agofou:

Average in-situ GPP -1.34 µmol CO2 m-2 sec-1

Convert it to g CO2 m-2 and s-1:

1 mol=44 g CO2 and micro=µ=10^{-6}

- ⇨ **Average in-situ GPP =0.000059 g CO2 m-2 s-1**

Convert it to g CO2 m-2 and 8 d-1:

8 days = (8*24*60*60) seconds

0.000059 g CO2 m-2 s-1 * (8*24*60*60)

- ⇨ **Average in-situ GPP =40.7 g CO2 m-2 and 8 day-1:**

Convert it to g C m-2 and 8 d-1:

1 g CO2 = 0.27 g C

Average in-situ GPP = 40.7*0.27= 11.0 g C m-2 and 8 day-1:

Average raw MODIS GPP for Agofou: 24.1

Scaling factor: 0.0001 =>

Modis GPP (kg C m-2 and 8 day-1)=0.00241 kg C m-2 and 8 day-1

Modis GPP (g C m-2 and 8 day-1)=0.00241 *1000 = 2.41 g C m-2 and 8 day-1.

Again, we agree that this major underestimation is strange, but we believe that all conversions are correctly done.

C. Minor Points

Line 42: While it is appropriate to mention that significant inter-annual variability in global carbon cycle arises in semi-arid regions relating to rainfall variability and fire (particularly in the mesic savannas, more so than the Sahel; eg. Williams et al Carbon Balance and Management 2007), it would be an exaggeration to state that the semiarid regions are "driving long-term trends".

Response: We agree with the reviewer that this was not a very clear sentence. But still, according (Ahlström et al., 2015) semi-arid region are driving the long term trends. We have clarified this in the revised manuscript:

"Vegetation growth in semi-arid regions is an important sink for fossil fuel emissions. Mean carbon dioxide (CO_2) uptake by terrestrial ecosystems is dominated by highly productive lands, mainly tropical forests, whereas semi-arid regions are the main biome driving its inter-annual variability (Ahlström et al., 2015; Poulter et al., 2014). Semi-arid regions even contribute to 60% of the long term trend in the global terrestrial C sink (Ahlström et al., 2015)."(L41-44)

Line 52: "continuous cropping" is very rare in the Sahel (outside of areas with irrigation opportunities, anyway). In the drier northern regions pastoralist communities may attempt a dryland crop, but with little expectation of success. Even in the wetter southern Sahel where the crop site in this paper is located, most fields are fallowed. In the highly populated regions near the capital city of Niger, rotations have reduced, but it would be wrong to imply that "continuous cropping is practiced" widely.

Response: Thank you for noticing this, this sentence has been removed.

Line 107: "find evidence" is awkward here. Perhaps substitute "characterize".

Response: Yes, we fully agree. Characterize is much better. Thank you very much.

References

Ahlström, A., Raupach, M. R., Schurgers, G., Smith, B., Arneth, A., Jung, M., Reichstein, M., Canadell, J. G., Friedlingstein, P., Jain, A. K., Kato, E., Poulter, B., Sitch, S., Stocker, B. D., Viovy, N., Wang, Y. P., Wiltshire, A., Zaehle, S., and Zeng, N.: The dominant role of semi-arid ecosystems in the trend and variability of the land CO_2 sink, Science, 348, 895-899, 10.1126/science.aaa1668, 2015.

Dardel, C., Kergoat, L., Hiernaux, P., Mougin, E., Grippa, M., and Tucker, C. J.: Re-greening Sahel: 30 years of remote sensing data and field observations (Mali, Niger), Remote Sens. Environ., 140, 350-364, http://dx.doi.org/10.1016/j.rse.2013.09.011, 2014.

ECMWF: ERA-Interim: surface photosynthetically active radiation (surface PAR) values are too low https://software.ecmwf.int/wiki/display/CKB/ERA-Interim%3A+surface+photosynthetically+active+radiation+%28surface+PAR%29+values+are+too+low, access: 7 November, 2016.

Hanan, N., Kabat, P., Dolman, J., and Elbers, J. A. N.: Photosynthesis and carbon balance of a Sahelian fallow savanna, Global Change Biol., 4, 523-538, 1998.

Hiernaux, P., Mougin, E., Diarra, L., Soumaguel, N., Lavenu, F., Tracol, Y., and Diawara, M.: Sahelian rangeland response to changes in rainfall over two decades in the Gourma region, Mali, J. Hydrol., 375, 114-127, http://dx.doi.org/10.1016/j.jhydrol.2008.11.005, 2009.

Mbow, C., Fensholt, R., Rasmussen, K., and Diop, D.: Can vegetation productivity be derived from greenness in a semi-arid environment? Evidence from ground-based measurements, J. Arid Environ., 97, 56-65, http://dx.doi.org/10.1016/j.jaridenv.2013.05.011, 2013.

Poulter, B., Frank, D., Ciais, P., Myneni, R. B., Andela, N., Bi, J., Broquet, G., Canadell, J. G., Chevallier, F., Liu, Y. Y., Running, S. W., Sitch, S., and van der Werf, G. R.: Contribution of semi-arid ecosystems to interannual variability of the global carbon cycle, Nature, 509, 600-603, 10.1038/nature13376, 2014.

Sager, J. C., and McFarlane, J. C.: Chapter 1. Radiation, in: Plant growth chamber handbook, edited by: W., L. R., and T.W., T., Iowa State University, Ames, 1997.

Tagesson, T., Fensholt, R., Guiro, I., Cropley, F., Horion, S., Ehammer, A., and Ardö, J.: Very high carbon exchange fluxes for a grazed semi-arid savanna ecosystem in West Africa, Danish Journal of Geography, 116, 93-109, http://dx.doi.org/10.1080/00167223.2016.1178072 2016.

Response to comments by Reviewer #2

General comments: This is an interesting paper providing detailed descriptions of spatial and temporal dynamics in canopy light-response parameters at CO_2 flux observation sites across Sahel region. The authors evaluated MODIS GPP, and reported its serious problem. This paper demonstrated the applicability of alternative model to scale up EC flux-based GPP to regional or continental scales, using EO-based spectral vegetation indices. The dynamics of photosynthetic parameters and some interpretations of several vegetation indices presented in this paper are valuable to estimate CO_2 budget in semi-arid ecosystems, which have included large uncertainties so far. Overall presentation is well structured and clear. The purpose of this paper fits well to this journal.

Response: Thank you very much, and also thank you for insightful comments that helped improving our manuscript.

Specific comments:
1. The intra-annual dynamics in F_{opt} and α were well explained with the vegetation indices in relation to the seasonal changes in water thickness and chlorophyll abundance. But the shorter term variations in F_{opt} and α (Fig. 4) do not seem to be explained sufficiently by the regression tree analysis. Some stress events may affect them. Please show the relationships with meteorological variables such as SWC or VPD additionally, and describe more information on the related specific stress events.

Response: We are truly sorry, but we do not completely agree. In Table 3, results from the regression trees are presented and the coefficient of determination (R^2) is larger than 0.9 for most sites; when all sites are combined it was 0.87 and 0.84 for F_{opt} and α respectively. So we would say that the regression trees describe the short term variability in F_{opt} and α pretty well. To further clarify this, we have incorporated a figure to the supplementary material with both measured and regression tree predicted F_{opt} and α. This indicates that SWC and VPD have a strong influence on the short term variability, since these explanatory variables are included in most regression trees (Table 3). This info is included in the revised manuscript (L232-239; L296-304; where L is line in revised manuscript).

2. The result of strong underestimation of ERA Interim PAR against in situ PAR is surprising and important information. Please confirm the ERA Interim PAR data: it is W m^{-2} (Line 157), but μmol m^{-2} s^{-1} (Fig.2). In addition, there seems to be some different tendencies in the relationships in Fig. 2, maybe depending on the periods and sites. Were the PAR sensors calibrated regularly? PAR sensors tend to deteriorate as aging. Please check the deterioration in PAR by comparison with the simultaneously measured Rg.

Response: We completely understand your concern regarding this relationship, and we were very concerned ourselves. 1) Regarding the in-situ PAR data; we agree, two PAR sensors standing next to each other can easily give quite different values, and some minor differences between in-situ PAR and ECMWF could possibly be explained by this issue. However, the sensors have been sent for calibration regularly, and they have been intercalibrated before and after each rainy season. So this should not be a major issue. The different tendencies seen is most likely related to the fact that ECMWF PAR is given in UTC time for each 3h. We converted this to local time when comparing against the in-situ data, and different periods of the day thereby might get slightly different tendencies in the relationship.

2) Regarding the unit conversions: we have been looking at these conversions many times to make absolutely sure that the conversions are correctly done:

The average raw in-situ PAR = 483 µmol m-2 s-1

The average raw ECMWF PAR = 350503 (J m-2 summed for 3 hours)

To get ECMWF PAR to (W m-2): raw ECMWF PAR was divided by (60sec*60 minutes*3 hours) =>
Average ECMWF PAR (W m-2) =350503/(60*60*3)= 32 W m-2.

To convert ECMWF PAR (W m-2) to µmol m-2 we multiplied with 4.57 (Sager and McFarlane, 1997):

Average ECMWF PAR (µmol m-2 s-1) =32*4.57= 148 µmol m-2 s-1

Average in-situ PAR (µmol m-2 s-1)/ Average ECMWF PAR (µmol m-2 s-1) = 483/148 = 3.2

So we think that the PAR conversion is correctly done. We recently found out that the issue is related to a major error in the code of ECMWF:
"The surface incident value (code 58) seems erroneously low. For example, in locations in the Celtic Sea, surface PAR is typically around 20% to 25% of the clear sky value (code 20), and about a third of in-situ measurement of surface PAR. Cause: We have shortwave bands that include 0.442-0.625 micron, 0.625-0.778 micron and 0.778-1.24 micron. PAR is coded as if it was intending to sum all of the radiation in the first of these and 0.42 of the second (to account for the fact that PAR is normally defined to stop at 0.7 microns. However, PAR is in fact calculated from the sum of the second band plus 0.42 of the third." (ECMWF, 2016).

This indicates that the ERA-interim surface PAR product is actually not PAR, but rather incoming red and near infrared. However, we still intend to use this data source since we relate the gridded ECMWF PAR to in-situ measured PAR and used this relationship to convert ECMWF PAR to the proper level. The relationship should be ok, even if it is relating in-situ PAR to a different part of the spectrum; the final product is still PAR at a reasonable level. The conversion of ERA interrim PAR is described in the revised manuscript (L207-214).

3. This paper aims to provide a model to scale up observed canopy scale GPP to regional or continental scales, using EO-based spectral vegetation indices. The readers will expect a final map of spatial distribution of GPP in semi-arid areas, and the map would make this paper more valuable.

Response: We agree with the reviewer, in the previous version we did not include the full gridded map because the spatial up-scaling requires some very heavy computer processing. However, we have now borrowed computer power from the university, and in the revised version of the manuscript we have included a full gridded map of average peak F_{opt}, average peak α and an average annual sum of GPP 2001-2014 (L322-L326; Fig. 5).

Minor comments:
Line 184: What do you mean by "air-water interface"?

Response: We agree that the formulation was not clear. This has been corrected in the revised manuscript:

“The NIR radiance is reflected by the leaf cells since an absorption of these wavelengths would result in overheating of the plant whereas red radiance is absorbed by chlorophyll and its accessory pigments (Gates et al., 1965).” (L177-178)

Table 2: Correlation between “intra-annual” dynamics

Response: Thank you for pointing this out. This has been taken care of.

Please unify the descriptions: use $F_{optfrac}$ and $\_{frac}$ for intra-annual dynamics instead F_{opt} and α in Table 2, 3, as described in the text.

Response: Thank you for pointing this out. The F_{opt} and α were not normalised to F_{opt_frac} and $\alpha_{\_frac}$ for all analysis, they were only normalised when the analysis was conducted for all sites. This has been clarified in the revised manuscript (L222-334). In Table 2 and 3, it has also been incorporated that it was F_{opt} and α for all single site analysis, whereas it was F_{opt_frac} and $\alpha_{\_frac}$ for all sites analysis.

Fig 3: Some points of ML-Kem are quite low (nearly 0) for MODIS GPP, while around 8 g C m-2 d-1 for EC GPP. Why?

Response: Kelma is an inundated Acacia forest located in a clay-soil depression. These differentiated values are from the beginning of the dry season, when the depression continues to have high CO_2 fluxes since it is still inundated, whereas, the larger area was turning dry. The EC based footprint covers this depression and in-situ GPP was thereby high, whereas the satellite based GPP covering the larger area estimated low values. This info is included in the revised manuscript (L275-278).

Please unify the descriptions: α instead of QE, as described in the text. Clarify the labels and scales on X-axes.

Response: We have now inserted α into the figures. Scales has been unified on the x-axis.

(f) What is the reason that VI decreased less than 0.15 before the growing season in 2007 at NE-WaM?

Response: There are two possible reasons: 1) Uncertainty in the remote sensing data. The end of the dry season and the beginning of the rainy season is the period of highest uncertainty in the satellite data due to aerosol and cloud contamination. This could possibly affect the VI to a low value. 2) Another possible explanation is that NE-WaM is a millet field. Agricultural practice is that before the rainy season farmers cut the shrubs in their fields. The fields are thereby cleared of vegetation before the sowing, which would decrease the VI substantially.

Modelling spatial and temporal dynamics of GPP in the Sahel from earth observation based photosynthetic capacity and quantum efficiency

Torbern Tagesson[1], Jonas Ardö[2], Bernard Cappelaere[3], Laurent Kergoat[4], Abdulhakim Abdi[2], Stéphanie Horion[1], Rasmus Fensholt[1]

[1]Department of Geosciences and Natural Resource Management, University of Copenhagen, Øster Voldgade 10, DK-1350 Copenhagen, Denmark; E-Mails: torbern.tagesson@geoign.ku.dk, stephanie.horion@ignogeo.ku.dk, rf@ignogeo.ku.dk

[2]Department of Physical Geography and Ecosystem Science, Lund University, Sölvegatan 12, SE- 223 62 Lund, Sweden, E-Mails: jonas.ardo@nateko.lu.se, hakim.abdi@gmail.com

[3]HydroSciences Montpellier, IRD, CNRS, Univ. Montpellier, Montpellier, France, E-Mail: bernard.cappelaere@um2.fr

[4]Geoscience Environnement Toulouse, (CNRS/UPS/IRD), 14 av E Belin, 31400 Toulouse, France, E-Mail: laurent.kergoat@get.obs-mip.fr

Correspondence to: Torbern Tagesson (torbern.tagesson@ign.ku.dk)

Abstract. It has been shown that vegetation growth in semi-arid regions is an important sink for human induced fossil fuel emissions for the variability of the global terrestrial CO_2 sink, which indicates the strong need for improved understanding, and spatially explicit estimates of CO_2 uptake (gross primary productivityproduction (GPP)) in semi-arid ecosystems. This study has three aims: 1) to evaluate the MOD17A2H GPP (collection 6) product against eddy covariance (EC) based GPP for six sites across the Sahel.-; 2) To to find evidence oncharacterise the relationships between spatial and temporal variability in EC based photosynthetic capacity (F_{opt}) and quantum efficiency (α) and earth observation (EO) based vegetation indices (normalized difference vegetation index (NDVI); renormalized difference vegetation index (RDVI); enhanced vegetation index (EVI); and shortwave infrared water stress index (SIWSI)); and 3) To to study the applicability of EO up-scaled F_{opt} and α for GPP modelling purposes. MOD17A2H GPP (collection 6) underestimated GPP strongly, most likely because the maximum light use efficiency is set too low for semi-arid ecosystems in the MODIS algorithm. The Iintra-annual dynamics in F_{opt} was closely related to the shortwave infrared water stress index (SIWSI) closely coupledbeing sensitive to equivalent water thickness, whereas α was closely related to the renormalized difference vegetation index (RDVI) affected by chlorophyll abundance. Spatial and inter-annual dynamics in F_{opt} and α were closely coupled to the normalized difference vegetation index (NDVI) and RDVI, respectively. Modelled GPP based on F_{opt} and α up-scaled using EO based indices reproduced in situ GPP well for all but except a cropped site. The cropped site that was strongly impacted by intensive anthropogenic land use. Up-scaled GPP for Sahel 2001-2014 was 736±39 g C m^{-2} y^{-1}. This study indicates the strong applicability of EO as a tool

for ~~parameterising~~ spatially explicit estimates of GPP, F_{opt} and α~~photosynthetic capacity and efficiency~~; incorporating EO-based F_{opt} and α ~~this in~~in to dynamic global vegetation models could improve global ~~estimations~~ estimates of vegetation ~~productivity~~production, ecosystem processes and biogeochemical and hydrological cycles.

Keywords: Remote sensing, Gross Primary Productivity, MOD17A2H, light use efficiency, photosynthetic capacity, quantum efficiency

1 Introduction

Vegetation growth in semi-arid regions is an important sink for ~~human induced~~ fossil fuel emissions. Mean carbon dioxide (CO_2) uptake by terrestrial ecosystems is dominated by highly productive lands, mainly tropical forests, whereas ~~Semi~~semi-arid regions are ~~even~~ the main biome driving ~~long-term trends and~~its ~~-~~inter-annual variability (Ahlström et al., 2015; Poulter et al., 2014). ~~in carbon dioxide (CO_2) uptake by terrestrial ecosystems~~ Semi-arid regions even contribute to 60% of the long term trend in the global terrestrial C sink (Ahlström et al., 2015). ~~(Ahlström et al., 2015; Poulter et al., 2014).~~ It is thus important to understand ~~the~~ long-term variability of vegetation growth in semi-arid areas and their response to environmental conditions to better quantify and forecast ~~the~~ effects of climate change.

~~The~~ Sahel is a semi-arid transition zone between the dry Sahara desert in the North and the humid Sudanian savanna in the ~~south~~South. The region has experienced numerous severe droughts during the last decades that resulted in region-wide famines in 1972-1973 and 1984–1985 and localized food shortages across the region in 1990, 2002, 2004, 2011 and 2012 (Abdi et al., 2014; United Nations, 2013). Vegetation ~~productivity~~ production is thereby an important ecosystem service for ~~the people living~~ livelihoodin ~~the~~ Sahel, but it is under ~~high pressure~~threat. The region experiences a strong population growth, increasing the demand on ~~the~~ ecosystem services due to cropland expansion, increased pasture stocking rates and fuelwood extraction (Abdi et al., 2014). ~~Continuous cropping is practised to meet the demand of the growing population and has resulted in reduced soil fertility, which affects vegetation productivity negatively (Samaké et al., 2005; Chianu et al., 2006).~~

At the same time as we have reports of declining vegetation ~~productivity~~production, we have contradicting reports of greening of the Sahel based on earth observation (EO) ~~remote sensing~~ data (Dardel et al., 2014; Fensholt et al., 2013). The greening of ~~the~~ Sahel has mainly been attributed to alleviated drought stress conditions due to increased precipitation since the mid-1990s (Hickler et al., 2005). Climate is thus another important factor regulating vegetation ~~productivity~~production. ~~S and s~~emi-arid regions, such as ~~the~~ Sahel, are particularly vulnerable to climate fluctuations due to their ~~vulnerability~~ dependency to moisture conditions.

Estimation of gross primary ~~productivity~~production (GPP), i.e. uptake of atmospheric CO_2 by vegetation, is still a major challenge within remote sensing of ecosystem services. ~~GPP~~ Gross primary production is a main driver of ecosystem services such as climate regulation, carbon (C) sequestration, C storage, food production, or livestock grassland production. Within ~~earth observation (~~EO~~)~~, spatial quantification of GPP generally involves light use efficiency (LUE), defined as the conversion efficiency ~~to convert~~of absorbed solar light into CO_2 uptake (Monteith, 1972, 1977). It has been shown that LUE varies in space and time due to factors such as plant functional type, drought and temperature, nutrient levels and physiological limitations of photosynthesis (Garbulsky et al., 2010; Paruelo et al., 2004; Kergoat et al., 2008). The LUE concept has been applied using various methods, either by using a biome-specific

Field Code Changed

Field Code Changed

LUE constant (Ruimy et al., 1994), or by modifying a maximum LUE using meteorological variables (Running et al., 2004).

An example of an LUE based model is the standard GPP product from the Moderate Resolution Imaging Spectroradiometer (MODIS) sensor (MOD17A2). Within the model, absorbed photosynthetically active radiation (PAR) is estimated as a product of the fraction of PAR absorbed by ~~the~~ green vegetation (FPAR from MOD15A2) multiplied with daily PAR from the meteorological data of the Global Modeling and Assimilation Office (GMAO). A set of maximum LUE parameters specified for each biome are extracted from a Biome Properties Look-Up Table (BPLUT). Then maximum LUE is modified depending on air temperature (T_{air}) and vapor pressure deficit (VPD) ~~levels~~ (Running et al., 2004). Sjöström et al. (2013) evaluated the MOD17A2 product (collection 5.1) for Africa, and showed that it ~~was underestimating~~underestimated GPP for semi-arid savannas in ~~the~~ Sahel. Explanations for this underestimation were that the assigned maximum LUE from ~~the~~ BPLUT ~~is~~ was set too low and uncertainties in the FPAR (MOD15A2) product. Recently, a new collection of MOD17A2 at 500 m spatial resolution was released (MOD17A2H; collection 6) with an updated BPLUT, updated GMAO meteorological data, improved quality control and gap filling of the FPAR data from MOD15A2 (Running and Zhao, 2015).

It has been shown that the LUE method does not perform well in arid conditions and at agricultural sites (Turner et al., 2005). Additionally, the linearity assumed by the LUE model is usually not found as the response of GPP to incoming light follows more of an asymptotic curve (Cannell and Thornley, 1998). Investigating other methods for remotely determining GPP is thus of great importance, especially for semi-arid environments. Therefore, instead of LUE we focus on the light response function of GPP at ~~the~~ canopy scale, and spatial and temporal variation of its two main parameters: maximum GPP under light saturation (canopy-scale photosynthetic capacity; F_{opt}), and the initial slope of the light response function (canopy-scale quantum efficiency; α) (Falge et al., 2001; Tagesson et al., 2015a). Photosynthetic capacity is a measure of the maximum rate at which the canopy can fix CO_2 during photosynthesis (μmol CO_2 m^{-2} s^{-1}) whereas α is the amount of CO_2 fixed per incoming PAR (μmol CO_2 μmol PAR^{-1}). Just to clarify the difference in LUE and α in this study; LUE (μmol CO_2 μmol $APAR^{-1}$) is the slope of a linear fit between CO_2 uptake and absorbed PAR, whereas α (μmol CO_2 μmol PAR^{-1}) is the initial slope of an asymptotic curve against incoming PAR.

It has been proven that F_{opt} and α are closely related to chlorophyll abundance due to their coupling with the electron transport rate (Ide et al., 2010). Additionally, in semi-arid ecosystems water availability is generally considered to be the main limiting factor affecting intra-annual dynamics of vegetation growth (Fensholt et al., 2013; Hickler et al., 2005; Tagesson et al., 2015b). Several remote sensing studies have established relationships between remotely sensed vegetation indices and ecosystem properties such as chlorophyll abundance and equivalent water thickness (Yoder and Pettigrew-Crosby, 1995; Fensholt and Sandholt, 2003). In this study we will analyse if EO vegetation indices can be used for up-scaling F_{opt} and α and investigate if this could offer a promising way to map GPP in semi-arid areas. This potential will be analysed by the use of detailed ground observations from six ~~different~~ eddy covariance (EC) flux tower~~measurement~~ sites ~~(eddy covariance flux towers)~~ across ~~the~~ Sahel.

The three aims of this study are:

1) To ~~evaluate the recently released MOD17A2H GPP (collection 6) product and to~~ investigate if the recently released MOD17A2H GPP (collection 6) product ~~it~~ is better at capturing GPP ~~levels~~ for ~~the~~ Sahel than collection 5.1. We hypothesise that MOD17A2H GPP (collection 6) product will estimate GPP well for the six

Sahelian ~~measurement~~ EC sites, because of ~~the~~ major changes done in comparison to collection 5.1 (Running and Zhao, 2015).

2) To ~~find evidence~~characterize ~~on~~ the relationships between spatial and temporal variability in F_{opt} and α and remotely sensed vegetation indices. We hypothesise that ~~remotely sensed~~EO vegetation indices that are closely related to chlorophyll abundance ~~can be used for quantifying~~will be most strongly coupled with spatial and inter-annual dynamics in F_{opt} and α~~.~~, whereas v~~V~~egetation indices closely related to equivalent water thickness will be most strongly coupled with ~~are closely linked to~~ intra-annual dynamics in F_{opt} and α across ~~the~~ Sahel.

3) To evaluate the applicability of a GPP model based on the light response function using ~~remotely sensed~~EO vegetation indices and incoming PAR as input data.

2 Materials and Methods

2.1 Site description

The Sahel stretches from the Atlantic Ocean in the west to the Red Sea in the east. The northern border towards ~~the~~ Sahara and the southern border towards the humid Sudanian Savanna are defined by the 150 and 700 mm isohytes, respectively (Fig. 1) (Prince et al., 1995). Tree and shrub canopy cover is now generally low (< 5%) and dominated by species of *Balanites*, *Acacia*, *Boscia* and *Combretaceae* (Rietkerk et al., 1996). Annual grasses such as *Schoenefeldia gracilis*, *Dactyloctenium aegypticum*, *Aristida mutabilis*, and *Cenchrus biflorus* dominate the herbaceous layer, but perennial grasses such as *Andropogon gayanus*, *Cymbopogon schoenanthus* can also be found (Rietkerk et al., 1996; de Ridder et al., 1982). From the FLUXNET database (Baldocchi et al., 2001)~~,~~ we selected the six available measurement sites with ~~eddy covariance~~EC based CO_2 flux data from ~~the~~ Sahel (Table 1; Fig. 1). The sites represent a variety of ~~the~~ ecosystems present in the region, from dry fallow bush savanna to seasonally inundated acacia forest. For a full description of the measurement sites, we refer to Tagesson et al. (2016a) and ~~the~~ references in Table 1.

<Table 1>

<Figure 1>

2.2 Data collection

2.2.1 Eddy covariance~~,~~ and hydro~~logical and~~ meteorological in situ data

Eddy covariance ~~(EC),~~ and hydrolo~~gical and~~ meteorological data originating from the years between 2005 and 2013 were collected from the principal investigators of the measurement sites (Tagesson et al., 2016a). The EC sensor set-up consisted of open-path CO_2/H_2O infrared gas analysers and 3-axis sonic anemometers. Data were collected at 20 Hz rate and statistics were calculated for 30-min periods. For a full description of sensor set up and post processing of ~~the~~ EC data, see references in Table 1. Final fluxes were filtered according to quality flags provided by FLUXNET and outliers were filtered according to Papale et al. (2006). We extracted the original net ecosystem exchange (NEE) data without any gap-filling or partitioning of NEE to GPP and ecosystem respiration. ~~We also~~The collected hydrolo~~gical and~~ meteorological data were: air temperature (T_{air}; °C), rainfall (P; mm), relative air humidity (Rh; %), soil moisture at 0.1 m depth (SWC; % volumetric water content), incoming global radiation (R_g; W m^{-2}), incoming photosynthetically active radiation (PAR; µmol m^{-2} s^{-1}), VPD (hPa), peak dry weight biomass (g dry weight m^{-2}), C3/C4 species ratio, and

soil conditions (nitrogen and C concentration; %). For a full description of ~~the~~ collected data and sensor set-up, see Tagesson et al. (2016a).

2.2.2 Earth Observation data and gridded ancillary data

~~Remotely sensed~~C ~~c~~omposite products from ~~the~~ MODIS/Terra ~~L4 from~~ covering ~~the~~ Sahel were ~~collected~~ acquired at Reverb ECHO (NASA, 2016). ~~The~~ Ccollected products were GPP (MOD17A2H; collection 6), ~~and the Nadir~~ nadir ~~Bidirectional~~ bidirectional ~~Reflectance~~ reflectance ~~Distribution~~ distribution ~~F~~function ~~(BRDF)~~ ~~adjusted~~ adjusted ~~reflectance~~ reflectance (NBAR) (8-day composites; MCD43A4; collection 5.1) at 500*500 m^2 spatial resolution, ~~and~~ the normalized difference vegetation index (NDVI)~~,~~ and the enhanced vegetation index (EVI) (16-day composites; MOD13Q1; collection 6) at 250*250 m^2 spatial resolution. The NBAR product was preferred over the reflectance product (MOD09A1), in order to avoid variability caused by varying sun and sensor viewing geometry (Huber et al., 2014; Tagesson et al., 2015c). We extracted the median of ~~the~~ 3x3 pixels centred at the location of ~~the~~ each EC tower~~s~~. ~~The~~ T~~t~~ime series of ~~the remotely sensed~~EO products were filtered according to ~~the~~ MODIS quality control data; MOD17A2H is a gap-filled and filtered product, QC data from MCD43A2 were used for ~~the~~ filtering of MCD43A4; and bit 2-5 (highest –decreasing quality) was used for MOD13Q1. Finally, data were gap-filled to daily values using linear interpolation.

~~For a GPP model to be applicable on a larger spatial scale, a gridded data set of incoming PAR is needed.~~ We downloaded ERA Interim reanalysis PAR at the ground surface (W m^{-2}) with a spatial resolution of 0.25°×0.25° accumulated for each 3-hour period 2000-2015 from the European Centre for Medium-Range Weather Forecasts (ECMWF) (Dee et al., 2011; ECMWF, 2016a).

2.3 Data handling

2.3.1 Intra-annual dynamics in photosynthetic capacity and quantum efficiency

~~Both linear and hyperbolic equations have been used for investigating the response of GPP to incoming light (Wall and Kanemasu, 1990; Campbell et al., 2001). However, they do not represent the lower part of the light response function particularly well, and we thereby instead choose to use the asymptotic Mitscherlich light response function (Inoue et al., 2008; Falge et al., 2001).~~ ~~The~~ To estimate daily values of EC based F_{opt} and α, the asymptotic Mitscherlich light-response function was fitted between daytime NEE and incoming PAR using a 7-day moving window with a 1-day time step:

$$NEE = -(F_{opt}) \times (1 - e^{\left(\frac{-\alpha \times PAR}{F_{opt}}\right)}) + R_d \quad (1)$$

where F_{opt} is ~~the~~ CO_2 uptake at light saturation (photosynthetic capacity; μmol CO_2 m^{-2} s^{-1}), R_d is dark respiration (μmol CO_2 m^{-2} s^{-1}), and α is the initial slope of the light response curve (quantum efficiency; μmol CO_2 μmol PAR^{-1}) (Falge et al., 2001). By subtracting R_d from Eq. 1, the function ~~is~~ was forced through zero and GPP ~~is~~ was thereby estimated. ~~We fitted Eq. 1 using 7-day moving windows with 1-day time steps and generating daily values of F_{opt} and α.~~ To assure high quality of ~~the~~ fitted parameters, parameters were excluded from the analysis when ~~the~~ fitting was insignificant (p-value ~~>~~ < 0.05), and when they were out of range (F_{opt} and α >peak value of the rainy season times 1.2).

Additionally, outliers were filtered following the method by Papale et al. (2006) using a 30-day moving windows with a 1- day time steps.

2.3.2 Vegetation indices

We analysed the relationship between F_{opt}, α and some commonly applied vegetation indices:

The maximum absorption in the red wavelengths generally occurs at 682 nm as this is the peak absorption for chlorophyll a and b (Thenkabail et al., 2000), which makes vegetation indices that include the red band sensitive to chlorophyll abundance. By far the most common vegetation index is the NDVI (Rouse et al., 1974):

$$NDVI = \frac{(\rho_{NIR} - \rho_{red})}{(\rho_{NIR} + \rho_{red})} \quad (2)$$

where ρ_{NIR} is the reflectance factor in the near infrared (NIR) band (band 2) and ρ_{red} is the reflectance factor in the red band (band 1). The Near infrared NIR radiance is scattered by the air-water interfaces between the cellsreflected by leaf cells since absorption of these wavelengths would result in overheating of the plant whereas red radiance is absorbed by chlorophyll and its accessory pigments (Gates et al., 1965). Normalization is done to reduce effects of atmospheric errors, solar zenith angles, and sensor viewing geometry, as well as increasing the vegetation signal (Qi et al., 1994; Inoue et al., 2008).

A well-known issue withdeficiency of the NDVI is that it saturatesproblems of index saturation at high biomass because the absorption of red light at ~670 nm peaks at higher biomass loads whereas NIR reflectance continues to increase due to multiple scattering effects (Mutanga and Skidmore, 2004; Jin and Eklundh, 2014). By reducing atmospheric and soil background influences, EVI is designed to increases the signal from the vegetation and maintain sensitivity in high biomass regions (Huete et al., 2002).

$$EVI = G\frac{(\rho_{NIR} - \rho_{red})}{(\rho_{NIR} + C_1\rho_{red} - C_2\rho_{blue} + L)} \quad (3)$$

where ρ_{blue} is the reflectance factor in the blue band (band 3). The coefficients C_1=6 and C_2=7.5 correct for atmospheric influences, while L=1 adjust for the canopy background. The factor G=2.5 is the a gain factor.

Another attempt to overcome the issueproblems of NDVI saturation was proposed by Roujean and Breon (1995), Roujean and Breon (1995) who suggested which the renormalized difference vegetation index (RDVI) that combines the advantages of the DVI (NIR-red) and the NDVI for low and high vegetation cover, respectively:

$$RDVI = \frac{(\rho_{NIR} - \rho_{red})}{\sqrt{(\rho_{NIR} + \rho_{red})}} \quad (4)$$

As a non-linear index, RDVI is not only less sensitive to variations in the geometrical and optical properties of unknown foliage but also less affected by the solar and viewing geometry (Broge and Leblanc, 2001). RDVI was calculated based on NBAR bands 1 and 2.

The NIR and SWIR bands are affected by the same ground properties, except that SWIR bands are also strongly sensitive to equivalent water thickness. Fensholt and Sandholt (2003) proposed a vegetation index, the shortwave infrared water stress index (SIWSI), using NIR and SWIR bands to estimate drought stress for vegetation in semi-arid environments:

$$SIWSI_{12} = \frac{(\rho_{NIR} - \rho_{SWIR12})}{(\rho_{NIR} + \rho_{SWIR12})} \quad (5)$$

$$SIWSI_{16} = \frac{(\rho_{NIR} - \rho_{SWIR16})}{(\rho_{NIR} + \rho_{SWIR16})} \quad (6)$$

where ρ_{swir12} is NBAR band 5 (1230-1250 nm) and ρ_{swir16} is NBAR band 6 (1628-1652 nm). As the vegetation water content increases, ~~the~~ reflectance in ~~the~~ SWIR decreases indicating that low and high SIWSI values point to sufficient water conditions and drought stress, respectively.

2.3.3 Incoming PAR across ~~the~~ Sahel

A modified version of the ERA Interim reanalysis PAR was used in the current study as an error in the code producing these PAR estimates was identified by the data distributor causing PAR values to be too low (ECMWF, 2016b). Accordingly, incoming PAR at the ground surface from ERA Interim was systematically underestimated even though it followed the pattern of PAR measured at the six Sahelian EC sites (Fig. S1 in supplementary material). In order to correct for this error, we fitted and applied an ordinary least square linear regression between in situ PAR and ERA Interim PAR (Fig. S1). The produced PAR from this relationship is at the same level as measured PAR in situ and should be at a correct level even though the original ERA Interim PAR is actually produced from the red and near infrared part of the spectrum.

~~Incoming PAR at the ground surface from ERA Interim followed the pattern of PAR measured at the six sites in situ closely, but it was systematically underestimated (Fig. in supplementary material2). An ordinary least square linear regression was thereby fitted between ERA Interim PAR and PAR measured in situ ($PAR_{in\ situ}$=3.09* $PAR_{ERA\ interim}$ +23.07; coefficient of determination (R^2)=0.93; n=37976). We therebyaThe regression line was used .~~

~~<Figure 2>~~

Formatted: Font: Not Bold

Formatted: Normal, Line spacing: single

2.4 Data analysis

2.4.1 Coupling temporal and spatial dynamics in photosynthetic capacity and quantum efficiency with explanatory variables

~~In a first step,~~T ~~t~~he coupling between intra-annual dynamics in F_{opt} and α and the vegetation indices for the different measurement sites were studied using Pearson correlation analysis. As part of the correlation analysis, we used bootstrap simulations with 200 iterations from which mean and standard deviation of the correlation coefficients were calculated (Richter et al., 2012). Relationships between intra-annual dynamics in F_{opt} and α and the vegetation indices for all sites combined were also analysed. In the analysis for all sites, data were normalised in order to avoid influence of ~~the~~ spatial and inter-annual variability. T, ~~t~~ime series of ratios of F_{opt} and α (F_{opt_frac} and α_{frac}) against the annual peak values (F_{opt_peak} and α_{peak}; see below for calculation of annual peak values) were estimated for all sites:

$$F_{opt\_frac} = \frac{F_{opt}}{F_{opt\_peak}} \quad (7)$$

$$\alpha_{frac} = \frac{\alpha}{\alpha_{peak}} \quad (8)$$

The same standardisation procedure was used for all vegetation indices (VI_{frac}):

$$VI_{frac} = \frac{VI}{VI_{peak}} \quad (9)$$

where VI_{peak} is the annual peak values of the vegetation indices (14 days running mean with highest annual value). ~~Such a standardisation gives fractions of how F_{opt}, α and VI varies over the season in relationship to the annual peak value, and it removes the spatial and inter-annual variation, and mainly intra-annual dynamics remains.~~ The coupling between α_{frac} and F_{opt_frac} and the different VI_{frac} were examined using Pearson correlation analysis for all sites.

~~The robustness of the correlation coefficients was estimated by using a bootstrap simulation with 200 iterations in the correlation analysis (Richter et al., 2012).~~

~~In order to investigate spatial and inter-annual variability in F_{opt} and α for the measurement sites, gaps needed to be filled.~~ Regression trees were used to fill gaps in the daily estimates of F_{opt} and α. One hundred tree sizes were chosen based on 100 cross validation runs, and these trees were then used for estimating ~~the~~ F_{opt} and α following the method in De'ath and Fabricius (2000). We used SWC, VPD, T_{air}, PAR, and the vegetation index with strongest correlation with intra-annual dynamics as explanatory variables in the analysis. In the analysis for all sites, the same standardisation procedure as done for F_{opt}, α, and the vegetation indices was done for the hydro~~logical and~~ meteorological variables. The 100 F_{opt} and α output subsets from the regression trees were averaged and used for filling ~~the~~ gaps in the times series of F_{opt} and α. From these time-series we estimated annual peak values of F_{opt} and α (F_{opt_peak} and α_{peak}) as the 14-day running mean with highest annual value.

~~To~~ investigate spatial and inter-annual variability in F_{opt} and α across the measurement sites of the Sahel, ~~annual peak values of F_{opt} and α (F_{opt_peak} and α_{peak}; 14 days running mean with highest annual value)~~ were correlated with the annual sum of P, yearly means of T_{air}, SWC, RH, VPD, R_g, annual peak values of biomass, soil nitrogen and C concentrations, C3/C4 ratio, and VI_{peak} using Pearson linear correlations. ~~Again, we used a bootstrap simulation methodology with 200 iterations in order to estimate the robustness of the correlations.~~

2.4.2 Parameterisation and evaluation of the GPP model and evaluation of the MODIS GPP

~~**The GPP model**~~

Based on Eq. 1 and ~~the~~ outcome of the statistical analysis previously described under subsection 2.4.1 (for results see subsect. 3.2), a model for estimating GPP across ~~the~~ Sahel was created:

$$GPP = -F_{opt} \times (1 - e^{\left(\frac{-\alpha \times PAR}{F_{opt}}\right)}) \quad (10)$$

~~The model is applicable for each point in space and time.~~ Firstly, F_{opt_peak} and α_{peak} were estimated spatially and inter-annually using linear regression functions fitted against the vegetation indices with ~~the~~ strongest relationships to spatial and inter-annual variability in F_{opt_peak} and α_{peak} for all sites~~:~~.

~~$$F_{opt\_peak} = k_{Fopt} \times NDVI_{peak} + m_{Fopt} \quad (11)$$~~

$$\alpha_{peak} = k_{\alpha} \times RDVI_{peak} + m_{\alpha} \quad (12)$$

where k_{Fopt} and k_{α} are the slopes of the lines and m_{Fopt} and m_{α} are the intercepts. Secondly, to estimate the F_{opt_frac} and α_{frac} for each day of the year, linear exponential regression functions were established for F_{opt_frac} and α_{frac} with the vegetation index with the strongest relationships to intra-annual variability of F_{opt_frac} and α_{frac} for all sites, as follows:. By combining these relationships,

$$F_{opt\_frac} = n_{Fopt} \times e^{\left(l_{Fopt} \times RDVI_{frac}\right)} \quad (13)$$

$$\alpha_{frac} = n_{\alpha} \times e^{\left(l_{\alpha} \times RDVI_{frac}\right)} \quad (14)$$

where l_{Fopt} and l_{α} are the slopes of the lines and n_{Fopt} and n_{α} are the intercepts. Eq. 11-14 provide the relationships to estimate F_{opt} and α can be calculated for any day of the year and for any point in space across the Sahel:

$$F_{opt} = F_{opt\_peak} \times F_{opt\_frac} = \left(k_{Fopt} \times NDVI_{peak} + m_{Fopt}\right)\left(n_{Fopt} \times e^{\left(l_{Fopt} \times RDVI_{frac}\right)}\right) \quad (15\,11)$$

$$\alpha = \alpha_{peak} \times \alpha_{frac} = \left(k_{\alpha} \times RDVI_{peak} + m_{\alpha}\right)\left(n_{\alpha} \times e^{\left(l_{\alpha} \times RDVI_{frac}\right)}\right) \quad (16\,12)$$

where k_{Fopt} and k_{α} are slopes and m_{Fopt} and m_{α} are intercepts of the linear regressions giving F_{opt_peak} and α_{peak}, respectively; l_{Fopt} and l_{α} are coefficients and n_{Fopt} and n_{α} are intercepts of the exponential regressions giving F_{opt_frac} and α_{frac}, respectively. Equation 15 11 and 16 12 can bewere put inserted into Eq. 10 and GPP is were thereafter thereby estimated as:

$$GPP = -\left(F_{opt\_peak} \times F_{opt\_frac}\right) \times \left(1 - e^{\left(\frac{-\left(\alpha_{peak} \times \alpha_{frac}\right) \times PAR}{F_{opt\_peak} \times F_{opt\_frac}}\right)}\right) = -\left(\left(k_{Fopt} \times NDVI_{peak} + m_{Fopt}\right)\left(n_{Fopt} \times e^{\left(l_{Fopt} \times RDVI_{frac}\right)}\right)\right) \times \left(1 - e^{\left(\frac{-\left(k_{\alpha} \times RDVI_{peak} + m_{\alpha}\right)\left(n_{\alpha} \times e^{\left(l_{\alpha} \times RDVI_{frac}\right)}\right) \times PAR}{\left(k_{Fopt} \times NDVI_{peak} + m_{Fopt}\right)\left(l_{Fopt} \times RDVI_{frac} + n_{Fopt}\right)}\right)}\right) \quad (17)$$

generating a final model as:

$$GPP = -\left(\left(k_{Fopt} \times NDVI_{peak} + m_{Fopt}\right)\left(n_{Fopt} \times e^{\left(l_{Fopt} \times RDVI_{frac}\right)}\right)\right) \times \left(1 - e^{\left(\frac{-\left(k_{\alpha} \times RDVI_{peak} + m_{\alpha}\right)\left(n_{\alpha} \times e^{\left(l_{\alpha} \times RDVI_{frac}\right)}\right) \times PAR}{\left(k_{Fopt} \times NDVI_{peak} + m_{Fopt}\right)\left(l_{Fopt} \times RDVI_{frac} + n_{Fopt}\right)}\right)}\right) \quad (18\,13)$$

2.4.3 Parameterisation and evaluation of modelled GPP and evaluation of the MODIS GPP product

A bootstrap simulation methodology with 200 iterations was used when fitting the least-square regression functions In for parameterisation of theorder to estimate the robustness of the GPP model and its parameters, we used a bootstrap simulation methodology when fitting the empirical relationships. We used 200 iterations and different measurement sites were used in the different runs when fitting the empirical relationships (Richter et al., 2012). For each of the iterations, some of the EC sites were included and some were left-out. The runsThe bootstrap simulations generated 200 sets of k_{Fopt}, k_{α}, m_{Fopt}, m_{α}, l_{Fopt}, l_{α}, n_{Fopt}, n_{α}slopes, intercepts, , and coefficient of determination (coefficients of determination (R^2)), from which the medians and the standard deviations were estimated. Possible errors (e.g. random

sampling errors, aerosols, electrical sensor noise, filtering and gap-filling errors, clouds, and satellite sensor degradation) can be present in both the predictor and the response variables. Hence, we selected reduced major axis ~~linear~~ regressions to account for errors in both predictor and response variables when fitting the regression functions. The regression models were validated against the left-out ~~subsamples~~ sites within the bootstrap simulation methodology by calculating the root-mean-square-error (RMSE), and by fitting an ordinary least squares linear regression between modelled and ~~in situ~~independent variables.

Similarly, the MODIS GPP product (MOD17A2H, collection 6) was evaluated against ~~in situ~~independent GPP from the EC sites by calculating RMSE, and by fitting an ordinary least squares linear regression.

3 Results

3.1 Evaluation of the MODIS GPP product

There was a strong linear relationship between the MODIS GPP product (MOD17A2H; collection 6) and ~~the~~ independent ~~in situ~~ GPP (slope 0.17; intercept 0.11 g C m^{-2} d^{-1}; R^2 0.69; n=598). However, MOD17A2H strongly underestimated ~~in situ~~independent GPP (Fig. 2~~3~~) resulting in high RMSE (2.69 g C m^{-2} d^{-1}). It can be seen that some points for the Kelma site were quite low for MOD17A2H, whereas they were relatively high for the independent GPP (Fig. 2). Kelma is an inundated Acacia forest located in a clay soil depression. These differentiated values were found in the beginning of the dry season, when the depression was still inundated, whereas the larger area was turning dry.

<Figure ~~3~~2>

3.2 Intra-annual dynamics in photosynthetic capacity and quantum efficiency

Intra-annual dynamics in F_{opt} and α differed in amplitude, but were otherwise similar across the measurement sites in ~~the~~ Sahel (Fig. 4~~3~~). There ~~is~~ was no green ground vegetation during the dry season, and the low photosynthetic activity ~~is~~ was due to few evergreen trees. This ~~results~~ resulted in low values for both F_{opt} and α during the dry season. The vegetation responded strongly to rainfall, and both F_{opt} and α increased during the early phase of the rainy season. Generally, F_{opt} peaked slightly earlier than α (average± 1 standard deviation: 7±10 days) (Fig. 4~~3~~).

<Figure ~~4~~3>

All vegetation indices described well intra-annual dynamics in F_{opt} ~~well~~ for all sites (Table 2). $SIWSI_{12}$ had the highest correlation for all sites except Wankama Millet, where it was RDVI. When all sites were combined, all indices described well seasonality in F_{opt} ~~well~~, but RDVI had the strongest correlation (Table 2).

~~The I~~intra-annual dynamics in α were also closely coupled to intra-annual dynamics in the vegetation indices for all sites (Table 2). For α, RDVI was the strongest index describing intra-annual dynamics, except for Wankama Fallow where it was EVI. When all sites were combined all indices described well intra-annual dynamics in α ~~well~~, but RDVI was still the index with ~~the~~ strongest relationship (Table 2).

<Table 2>

The regression trees used for gap-filling explained well the ~~the~~ intra-annual dynamics in F_{opt} and α ~~well~~ for all sites (Table 3; Fig. S2 in Supplementary material). The regression trees explained intra-annual dynamics in F_{opt} better than in α, and multi-year sites were better predicted than single year sites (Fig. S2). The main explanatory variables coupled to

intra-annual dynamics in F_{opt} for all sites across ~~the~~ Sahel were in the order of RDVI, SWC, VPD, T_{air}, and PAR; and for α they were RDVI, SWC, VPD and T_{air} (Table 3). The strong relationship to SWC and VPD indicates drought stress during periods of low rainfall. For all sites across Sahel, incorporating hydro~~logical and~~ meteorological variables increased the ability to determine intra-annual dynamics in F_{opt} and α compared to the ordinary least squares linear regressions against ~~the RDVI~~vegetation indices (Table 2, data given as *r;* Table 3; Fig. 3 and Fig. S2). For all sites, ~~The~~ incorporation of these variables increased ~~the~~ R^2 from 0.81 to 0.87 and from 0.74 to 0.84, for F_{opt} and α respectively.

<Table 3>

3.3 Spatial and inter-annual dynamics in photosynthetic capacity and quantum efficiency

Large spatial and inter-annual variability in F_{opt_peak} and α_{peak} were found across the six measurement sites in ~~the~~ Sahel~~.~~; F_{opt_peak} ranged between 10.1 µmol CO_2 m^{-2} s^{-1} (Wankama_Millet 2005) and 50.0 µmol CO_2 m^{-2} s^{-1} (Dahra 2010), and α_{peak} ranged between 0.020 µmol CO_2 µmol PAR^{-1} (Demokeya 2007) and 0.064 µmol CO_2 µmol PAR^{-1} (Dahra 2010) (Table 4). The average two week running mean peak values of F_{opt} and α for all sites were 26.4 µmol CO_2 m^{-2} s^{-1} and 0.040 µmol CO_2 µmol PAR^{-1}, respectively. ~~However, the ranges were large; F_{opt_peak} ranged between 10.1 µmol CO_2 m^{-2} s^{-1} (Wankama_Millet 2005) and 50.0 µmol CO_2 m^{-2} s^{-1} (Dahra 2010), and α_{peak} ranged between 0.020 µmol CO_2 µmol PAR^{-1} (Demokeya 2007) and 0.064 µmol CO_2 µmol PAR^{-1} (Dahra 2010) (Table 4).~~ All vegetation indices determined well spatial and inter-annual dynamics in F_{opt_peak} and α_{peak} ~~well~~ (Table 5). $NDVI_{peak}$ was most closely coupled with F_{opt_peak} whereas $RDVI_{peak}$ was closest coupled with α_{peak} (Fig. ~~5~~4). F_{opt_peak} also correlated well with peak dry weight biomass, C content in the soil, and RH, whereas α_{peak} also correlated well with peak dry weight biomass, and C content in the soil (Table 5).

<Table 4>

<Table 5>

<Figure ~~5~~4>

3.4 Spatially extrapolated photosynthetic capacity, quantum efficiency, and gross primary ~~productivity~~**production** across ~~the~~ Sahel and evaluation of the GPP model

The spatially extrapolated F_{opt}, α and GPP averaged over Sahel for 2001-2014 were 22.5±1.7 µmol CO_2 m^{-2} s^{-1}, 0.030±0.002 µmol CO_2 µmol PAR^{-1}, and 736±39 g C m^{-2} y^{-1}, respectively. At regional scale it can be seen that F_{opt}, α, and GPP decreased substantially with latitude (Fig. 5). Highest values were found in south-eastern Senegal, western Mali, in parts of southern Sudan and on the border between Sudan and South Sudan. ~~(Brandt et al., 2016)~~Lowest values were found along the northernmost parts of Sahel on the border to Sahara in Mauritania, in northern Mali, and in northern Niger.

Modelled GPP was similar to in~~situ~~dependent GPP on average, and there was a strong linear relationship between modelled GPP and independent ~~situ~~ GPP for all sites (Fig. 6; Table 6). ~~–~~ However, when separating the evaluation between measurement sites, it can be seen that the model reproduced some sites better than others (Fig. 7; Table 6). Wankama Millet ~~is~~ was generally overestimated whereas the model ~~works~~ worked well on average ~~well~~ for Demokeya but ~~underestimates~~ underestimated high values (Fig. 7; Table 6). Variability of independent ~~situ~~ GPP at the other sites ~~is~~ was well reproduced by the model (Fig. 7; Table 6). ~~-~~The final parameters of the GPP model (Eq. ~~18~~13) are given in Table 7.

<Figure 5>

<Figure 6>

<Figure 7>

< Table 6>

< Table 7>

4 Discussion

~~Vegetation productivity of semi-arid savanna ecosystems is primarily driven by intra-annual rainfall distribution (Eamus et al., 2013; Brümmer et al., 2008; Moncrieff et al., 1997), and in the Sahel soil moisture conditions at the early rainy season are especially important (Rockström and de Rouw, 1997; Tagesson et al., 2016a; Mbow et al., 2013). We thereby hypothesised that vegetation indices closely related to equivalent water thickness (SIWSI) would be strongly linked to intra-annual dynamics in F_{opt} and α.~~ Our hypothesis that vegetation indices closely related to equivalent water thickness (SIWSI) would be most strongly coupled with intra-annual dynamics in F_{opt} and α was not rejected for F_{opt}, since this was ~~also~~ the case for all sites except for Wankama Millet (Table 2). ~~The Wankama millet is a cropped agricultural site whereas all other sites are savanna ecosystems.~~ However, our hypothesis was rejected for α, since it was more closely related to vegetation indices related to chlorophyll abundance (RDVI and EVI). ~~Leaf area index increases over the growing season and it is closely related to the vegetation indices coupled with chlorophyll abundance (Tagesson et al., 2009). This increases the canopy level quantum efficiency (α) which explains the close relationship of α to RDVI. However, F_{opt} peaked earlier in the rainy season than α (Fig. 4).~~ In Sahel, soil moisture conditions in the early rainy season are important for vegetation growth and during this phase vegetation is especially vulnerable to drought conditions (Rockström and de Rouw, 1997; Tagesson et al., 2016a; Mbow et al., 2013). Photosynthetic capacity (F_{opt}) peaked earlier in the rainy season than α did (Fig. 3), thereby explaining the close relationship of F_{opt} to SIWSI. Leaf area index increased over the growing season and leaf area index is closely coupled with vegetation indices related to chlorophyll abundance (Tagesson et al., 2009). The increase in leaf area index increased canopy level quantum efficiency (α), which thereby explains the closer relationship of α to RDVI. ~~Vegetation during this phase is vulnerable to drought conditions explaining the close relationship of F_{opt} to SIWSI. F_{opt} can only increase up to a certain level due to other constraining factors (nutrient, water and meteorological conditions) which could explain its closer relationship with $SIWSI_{12}$ than with RDVI.~~

Our hypothesis that vegetation indices closely related to chlorophyll abundance would be most strongly coupled with spatial and inter-annual dynamics in F_{opt} and α was not rejected for either F_{opt} or α; NDVI, EVI, and RDVI all had close correlation with spatial and inter-annual dynamics in F_{opt} and α (Table 5). However, i~~We hypothesised that remotely sensed vegetation indices closely related to chlorophyll abundance can be used for quantifying spatial and inter-annual dynamics in F_{opt} and α. Indeed, NDVI, EVI, and RDVI all had close correlations with the spatial and inter-annual dynamics in F_{opt} and α (Table 5).~~ It was surprising that $NDVI_{peak}$ had the strongest correlation with spatial and inter-annual variability for F_{opt} (Table 5). Both EVI and RDVI should be less sensitive to saturation effects than NDVI (Huete et al., 2002; Roujean and Breon, 1995), and based on this ~~we~~ it can be assumed that peak values of these indices should have stronger relationships to peak values of F_{opt} and α. However, vegetation indices with a high sensitivity to changes in green biomass at high biomass loads, gets less sensitive to green biomass changes at low biomass loads (Huete et al.,

Field Code Changed

Field Code Changed

2002). Peak leaf area index for ecosystems across ~~the~~ Sahel is ~~approximately~~ generally ~2 or less, whereas the saturation issue of NDVI generally starts at an leaf area index of about 2-5 (Haboudane et al., 2004).

Field Code Changed

The F_{opt_peak} estimates from Agoufou, Demokeya, and the Wankama sites were similar whereas Dahra and Kelma values were high in relation to previously reported canopy-scale F_{opt_peak} from Sahel (~-8 to -23 µmol m^{-2} sec^{-1}) (Hanan et al., 1998; Merbold et al., 2009; Moncrieff et al., 1997; Boulain et al., 2009; Levy et al., 1997; Monteny et al., 1997). These previous studies reported much lower F_{opt} at canopy scale than at leaf scale (e.g. Levy et al. (1997): 10 vs. 44 µmol m^{-2} sec^{-1}; Boulain et al. (2009): 8 vs. 50 µmol m^{-2} sec^{-1}). Leaf area index at Dahra and Kelma peaked at 2.1 and 2.7, respectively (Timouk et al., 2009; Tagesson et al., 2015a), and it was substantially higher than at the above-mentioned sites. A possible explanation to high F_{opt} estimates at Dahra and Kelma could thereby be the higher leaf area index. Tagesson et al. (2016b) performed a quality check of the EC data due to the high net CO_2 exchange measured at the Dahra field site and explained the high values by a combination of moderately dense herbaceous C4 ground vegetation, high soil nutrient availability, a grazing pressure resulting in compensatory growth and fertilization effects. Another possible explanation could be that the West African Monsoon bring a humid layer of surface air from the Atlantic, possibly increasing vegetation production for the most western part of Sahel (Tagesson et al., 2016a).

~~Additionally, atmospheric scattering is much higher in the shorter wavelengths making EO-based vegetation indices including blue band information very sensitive to the atmospheric correction (Fensholt et al., 2006b), possibly explaining the lower correlation for EVI.~~(Hanan et al., 1998; Merbold et al., 2009; Moncrieff et al., 1997; Boulain et al., 2009; Levy et al., 1997; Monteny et al., 1997; Timouk et al., 2009; Tagesson et al., 2015a); Tagesson et al. (2016b); (Tagesson et al., 2016a) Our model substantially ~~overestimates~~ overestimated GPP for Wankama Millet (Fig. 7f). ~~As a~~Being a crop field, this site ~~differs~~ differed ~~in particular~~ from the other studied sites by its species composition, ecosystem structure, as well as land and vegetation management. Crop fields in southwestern Niger are generally characterized by a rather low ~~productivity~~production resulting from decreased fertility and soil loss caused by intensive land use (Cappelaere et al., 2009). These specifics of the Wankama Millet site may cause the model parameterised with observations from the other study sites without this strong anthropogenic influence to overestimate GPP at this site. ~~The model parameterised using observation from the other measurement sites without this strong anthropogenic influence thus overestimates GPP.~~ Similar results were found by Boulain et al. (2009) when applying an up-scaling model using leaf area index for Wankama Millet and Wankama Fallow. It worked well for Wankama fallow whereas it was less conclusive for Wankama Millet. The main explanation was low leaf area index in millet fields because of a low density of millet stands due to agricultural practice. There is extensive savanna clearing for food production in ~~the~~ Sahel (Leblanc et al., 2008; Boulain et al., 2009; Cappelaere et al., 2009). To further understand ~~the~~ impacts of this land cover change on vegetation ~~productivity~~production and land atmosphere exchange processes, it is of urgent need for more study sites covering cropped areas in this region.

In Demokeya, GPP ~~is~~ was slightly underestimated for the year 2008 (Fig. 7c) because modelled F_{opt} ~~(the thick black line in Fig. 5) is~~ was much lower than the actual measured value in 2008 (the thick black line in Fig. 4). An improvement of the model could be to incorporate some parameters that constrain or enhance F_{opt} depending on environmental stress. Indeed, the regression tree analysis indicated that incorporating ~~climatic and~~ hydrometeorological variables increased the ability to predict both F_{opt} and α. On the other hand, for spatial upscaling purposes, it has been shown that including modelled hydrometeorological ~~climatic~~ constraints on LUE decreases the ability to predict

vegetation ~~productivity~~production due to the incorporated uncertainty in these modelled ~~meteorological~~ variables (Fensholt et al., 2006; Ma et al., 2014). For spatial upscaling to regional scales it is therefore better to simply use relationships to EO data. This is particularly the case for ~~the~~ Sahel, one of the largest dryland areas in the world that ~~is characterised by~~includes only a few sites of hydrometeorological ~~meteorological~~ observations.

The pattern seen in the spatially explicit GPP budgets (Fig. 5c) may be influenced by a range of biophysical and anthropogenic factors. The clear North-South gradient is expected given the strong North-South rainfall gradient in Sahel. The West African Monsoon mentioned above could also be an explanation to high GPP values in the western part of Sahel, where values were relatively high in relation to GPP at similar latitudes in the central and eastern Sahel (Fig. 5c). The areas with highest GPP are sparsely populated woodlands or shrubby savanna with a relatively dense tree cover (Brandt et al., 2016). However, the produced maps should be used with caution as they are based on up-scaling of the only six available EC sites that exist in the region; especially given the issues related to the cropped fields discussed above. Still, the average GPP budget for the entire Sahel 2001-2014 was close to an average annual GPP budget as estimated for these six sites (692±89 g C m^{-2} y^{-1}) (Tagesson et al., 2016a). The range of GPP budgets in Fig. 5c is also similar to previous annual GPP budgets reported from other savanna areas across the world (Veenendaal et al., 2004; Chen et al., 2003; Kanniah et al., 2010; Chen et al., 2016).

Although MOD17A2 GPP has previously been shown to relatively well capture GPP ~~relatively well~~ in several different ecosystems (Turner et al., 2006; Turner et al., 2005; Heinsch et al., 2006; Sims et al., 2006; Kanniah et al., 2009), it has been shown to be underestimated for others (Coops et al., 2007; Gebremichael and Barros, 2006; Sjöström et al., 2013). GPP of Sahelian drylands have not been well captured by MOD17A2 (Sjöström et al., 2013; Fensholt et al., 2006), and as we have shown, this underestimation persists in the latest MOD17A2H GPP (collection 6) product (Fig. 2). The main reason for this ~~major~~ pronounced underestimation is that maximum LUE is set to 0.84 g C MJ^{-1} (open shrubland; Demokeya) and 0.86 g C MJ^{-1} (grassland; Agoufou, Dahra, Kelma; Wankama Millet and Wankama Fallow) in the BPLUT, i.e. much lower than maximum LUE measured at the Sahelian measurement sites of this study (average: 2.47 g C MJ^{-1}; range: 1.58-3.50 g C MJ^{-1}) (Sjöström et al., 2013; Tagesson et al., 2015a), a global estimate of ~1.5 g C MJ^{-1} (Garbulsky et al., 2010), and a savanna site in Australia (1.26 g C MJ^{-1}) (Kanniah et al., 2009).

Several ~~state of the art~~ dynamic global vegetation models have been used for decades to quantify GPP at different spatial and temporal scales (Dickinson, 1983; Sellers et al., 1997). These models are generally based on the photosynthesis model by Farquhar et al. (1980), a model particularly sensitive to uncertainty in photosynthetic capacity (Zhang et al., 2014). This and several previous studies have shown that both photosynthetic capacity and efficiency (both α and LUE) can ~~considerably~~ vary considerably between season~~ally as well as and~~ spatially, and both within and between vegetation types (Eamus et al., 2013; Garbulsky et al., 2010; Ma et al., 2014; Tagesson et al., 2015a). This variability is difficult to estimate using broad values based on land cover classes, yet most models apply a constant value which can cause substantial inaccuracies in the estimates of seasonal and spatial variability in GPP. This is particularly a problem in savannas that comprises ~~of~~ several plant functional types (C3 and C4 species, and a large variability in tree/herbaceous vegetation fractions) (Scholes and Archer, 1997). This study indicates the strong applicability of EO as a tool for parameterising spatially explicit estimates of plant physiological variables, which could improve our ability to simulate GPP. Spatially explicit estimates of GPP at a high temporal and spatial resolution are essential for ~~current global~~environmental change studies in Sahel and ~~would be~~make a major asset for ~~advantageous in~~

511 the analysis of changes in GPP, its relationship to climatic change and anthropogenic forcing, and estimations of
512 ecosystem processes and biochemical and hydrological cycles.
513
514 **Acknowledgements** Data is available from Fluxnet (http://fluxnet.ornl.gov) and CarboAfrica
515 (http://www.carboafrica.net/index en.asp). Data for the Mali and Niger sites were made available by the AMMA-
516 CATCH regional observatory (www.amma-catch.org), which is funded by the French Institut de Recherche pour le
517 Développement (IRD) and Institut National des Sciences de l'Univers (INSU). The project was funded by the Danish
518 Council for Independent Research (DFF) Sapere Aude programme. Faculty of Science, Lund University supported the
519 Dahra and Demokeya measurements with an infras-tructure grant. Ardö received support from the Swedish National
520 Space Board.
521
522 **References**
523 Abdi, A., Seaquist, J., Tenenbaum, D., Eklundh, L., and Ardö, J.: The supply and demand of net
524 primary production in the Sahel, Environ. Res. Lett., 9, 094003, doi:10.1088/1748-9326/9/9/094003,
525 2014.
526 Ahlström, A., Raupach, M. R., Schurgers, G., Smith, B., Arneth, A., Jung, M., Reichstein, M.,
527 Canadell, J. G., Friedlingstein, P., Jain, A. K., Kato, E., Poulter, B., Sitch, S., Stocker, B. D., Viovy,
528 N., Wang, Y. P., Wiltshire, A., Zaehle, S., and Zeng, N.: The dominant role of semi-arid ecosystems
529 in the trend and variability of the land CO_2 sink, Science, 348, 895-899, 10.1126/science.aaa1668,
530 2015.
531 Baldocchi, D., Falge, E., Gu, L., Olson, R., Hollinger, D., Running, S., Anthoni, P., Bernhofer, C.,
532 Davis, K., Evans, R., Fuentes, J., Goldstein, A., Katul, G., Law, B., Lee, X., Malhi, Y., Meyers, T.,
533 Munger, W., Oechel, W., Paw, K. T., Pilegaard, K., Schmid, H. P., Valentini, R., Verma, S., Vesala,
534 T., Wilson, K., and Wofsy, S.: FLUXNET: A New Tool to Study the Temporal and Spatial
535 Variability of Ecosystem–Scale Carbon Dioxide, Water Vapor, and Energy Flux Densities, Bull.
536 Am. Meteorol. Soc., 82, 2415-2434, 10.1175/1520-0477(2001)082<2415:fantts>2.3.co;2, 2001.
537 Boulain, N., Cappelaere, B., Ramier, D., Issoufou, H. B. A., Halilou, O., Seghieri, J., Guillemin, F.,
538 Oï, M., Gignoux, J., and Timouk, F.: Towards an understanding of coupled physical and biological
539 processes in the cultivated Sahel – 2. Vegetation and carbon dynamics, J. Hydrol., 375, 190-203,
540 10.1016/j.jhydrol.2008.11.045, 2009.
541 Brandt, M., Hiernaux, P., Rasmussen, K., Mbow, C., Kergoat, L., Tagesson, T., Ibrahim, Y. Z.,
542 Wélé, A., Tucker, C. J., and Fensholt, R.: Assessing woody vegetation trends in Sahelian drylands
543 using MODIS based seasonal metrics, Remote Sens. Environ., 183, 215-225,
544 http://dx.doi.org/10.1016/j.rse.2016.05.027, 2016.
545 Broge, N. H., and Leblanc, E.: Comparing prediction power and stability of broadband and
546 hyperspectral vegetation indices for estimation of green leaf area index and canopy chlorophyll
547 density, Remote Sens. Environ., 76, 156-172, http://dx.doi.org/10.1016/S0034-4257(00)00197-8,
548 2001.
549 Cannell, M., and Thornley, J.: Temperature and CO_2 Responses of Leaf and Canopy Photosynthesis:
550 a Clarification using the Non-rectangular Hyperbola Model of Photosynthesis, Ann. Bot., 82, 883-
551 892, 1998.
552 Cappelaere, B., Descroix, L., Lebel, T., Boulain, N., Ramier, D., Laurent, J. P., Favreau, G.,
553 Boubkraoui, S., Boucher, M., Bouzou Moussa, I., Chaffard, V., Hiernaux, P., Issoufou, H. B. A., Le
554 Breton, E., Mamadou, I., Nazoumou, Y., Oi, M., Ottlé, C., and Quantin, G.: The AMMA-CATCH
555 experiment in the cultivated Sahelian area of south-west Niger – Investigating water cycle response

to a fluctuating climate and changing environment, J. Hydrol., 375, 34-51, 10.1016/j.jhydrol.2009.06.021, 2009.
Chen, C., Cleverly, J., and Zhang, L.: Modelling Seasonal and Inter-annual Variations in Carbon and Water Fluxes in an Arid-Zone Acacia Savanna Woodland, 1981–2012, Ecosystems, 19, 625-644, 2016.
Chen, X., Hutley, L., and Eamus, D.: Carbon balance of a tropical savanna of northern Australia., Oecologia, 137, 405-416, 2003.
Coops, N. C., Black, T. A., Jassal, R. S., Trofymow, J. A., and Morgenstern, K.: Comparison of MODIS, eddy covariance determined and physiologically modelled gross primary production (GPP) in a Douglas-fir forest stand, Remote Sens. Environ., 107, 385-401, http://dx.doi.org/10.1016/j.rse.2006.09.010, 2007.
Dardel, C., Kergoat, L., Hiernaux, P., Mougin, E., Grippa, M., and Tucker, C. J.: Re-greening Sahel: 30 years of remote sensing data and field observations (Mali, Niger), Remote Sens. Environ., 140, 350-364, http://dx.doi.org/10.1016/j.rse.2013.09.011, 2014.
De'ath, G., and Fabricius, K. E.: Classification and regression trees: A powerful yet simple technique for ecological data analysis, Ecology, 81, 3178-3192, 10.2307/177409, 2000.
de Ridder, N., Stroosnijder, L., and Cisse, A. M.: Productivity of Sahelian rangelands : a study of the soils, the vegetations and the exploitation of that natural resource, PPS course book. Primary Production in the Sahel, Agricultural University, Wageningen, 1982.
Dee, D. P., Uppala, S. M., Simmons, A. J., Berrisford, P., Poli, P., Kobayashi, S., Andrae, U., Balmaseda, M. A., Balsamo, G., Bauer, P., Bechtold, P., Beljaars, A. C. M., van de Berg, L., Bidlot, J., Bormann, N., Delsol, C., Dragani, R., Fuentes, M., Geer, A. J., Haimberger, L., Healy, S. B., Hersbach, H., Hólm, E. V., Isaksen, L., Kållberg, P., Köhler, M., Matricardi, M., McNally, A. P., Monge-Sanz, B. M., Morcrette, J. J., Park, B. K., Peubey, C., de Rosnay, P., Tavolato, C., Thépaut, J. N., and Vitart, F.: The ERA-Interim reanalysis: configuration and performance of the data assimilation system, Q. J. Roy. Meteor. Soc., 137, 553-597, 10.1002/qj.828, 2011.
Dickinson, R. E.: Land Surface Processes and Climate—Surface Albedos and Energy Balance, in: Advances in Geophysics, edited by: Barry, S., Elsevier, 305-353, 1983.
Eamus, D., Cleverly, J., Boulain, N., Grant, N., Faux, R., and Villalobos-Vega, R.: Carbon and water fluxes in an arid-zone Acacia savanna woodland: An analyses of seasonal patterns and responses to rainfall events, Agric. For. Meteorol., 182–183, 225-238, http://dx.doi.org/10.1016/j.agrformet.2013.04.020, 2013.
ECMWF: ERA Interim Daily: http://apps.ecmwf.int/datasets/data/interim-full-daily/levtype=sfc/, access: 04-04-2016, 2016a.
ECMWF: ERA-Interim: surface photosynthetically active radiation (surface PAR) values are too low https://software.ecmwf.int/wiki/display/CKB/ERA-Interim%3A+surface+photosynthetically+active+radiation+%28surface+PAR%29+values+are+too+low, access: 7 November, 2016b.
Falge, E., Baldocchi, D., Olson, R., Anthoni, P., Aubinet, M., Bernhofer, C., Burba, G., Ceulemans, R., Clement, R., Dolman, H., Granier, A., Gross, P., Grunwald, T., Hollinger, D., Jensen, N. O., Katul, G., Keronen, P., Kowalski, A., Lai, C. T., Law, B. E., Meyers, T., Moncrieff, J. B., Moors, E., Munger, J. W., Pilegaard, K., Rannik, U., Rebmann, C., Suyker, A., Tenhunen, J., Tu, K., Verma, S., Vesala, T., Wilson, K., and Wofsy, S.: Gap filling strategies for defensible annual sums of net ecosystem exchange, Agric. For. Meteorol., 107, 43-69, 2001.
Farquhar, G. D., Caemmerer, S., and Berry, J. A.: A biochemical model of photosynthetic CO_2 assimilation in leaves of C3 plants, Planta, 149, 78-90, 1980.

602 Fensholt, R., and Sandholt, I.: Derivation of a shortwave infrared water stress index from MODIS
603 near- and shortwave infrared data in a semiarid environment, Remote Sens. Environ., 87, 111-121,
604 http://dx.doi.org/10.1016/j.rse.2003.07.002, 2003.
605 Fensholt, R., Sandholt, I., Rasmussen, M. S., Stisen, S., and Diouf, A.: Evaluation of satellite based
606 primary production modelling in the semi-arid Sahel, Remote Sens. Environ., 105, 173-188,
607 10.1016/j.rse.2006.06.011, 2006.
608 Fensholt, R., Rasmussen, K., Kaspersen, P., Huber, S., Horion, S., and Swinnen, E.: Assessing Land
609 Degradation/Recovery in the African Sahel from Long-Term Earth Observation Based Primary
610 Productivity and Precipitation Relationships, Remote Sensing, 5, 664-686, 2013.
611 Garbulsky, M. F., Peñuelas, J., Papale, D., Ardö, J., Goulden, M. L., Kiely, G., Richardson, A. D.,
612 Rotenberg, E., Veenendaal, E. M., and Filella, I.: Patterns and controls of the variability of radiation
613 use efficiency and primary productivity across terrestrial ecosystems, Global Ecol. Biogeogr., 19,
614 253-267, 10.1111/j.1466-8238.2009.00504.x, 2010.
615 Gates, D. M., Keegan, H. J., Schleter, J. C., and Weidner, V. R.: Spectral Properties of Plants, Appl.
616 Optics, 4, 11-20, 1965.
617 Gebremichael, M., and Barros, A. P.: Evaluation of MODIS Gross Primary Productivity (GPP) in
618 tropical monsoon regions, Remote Sens. Environ., 100, 150-166,
619 http://dx.doi.org/10.1016/j.rse.2005.10.009, 2006.
620 Haboudane, D., Miller, J. R., Pattey, E., Zarco-Tejada, P. J., and Strachan, I. B.: Hyperspectral
621 vegetation indices and novel algorithms for predicting green LAI of crop canopies: Modeling and
622 validation in the context of precision agriculture, Remote Sens. Environ., 90, 337-352,
623 http://dx.doi.org/10.1016/j.rse.2003.12.013, 2004.
624 Hanan, N., Kabat, P., Dolman, J., and Elbers, J. A. N.: Photosynthesis and carbon balance of a
625 Sahelian fallow savanna, Global Change Biol., 4, 523-538, 1998.
626 Heinsch, F. A., Maosheng, Z., Running, S. W., Kimball, J. S., Nemani, R. R., Davis, K. J., Bolstad,
627 P. V., Cook, B. D., Desai, A. R., Ricciuto, D. M., Law, B. E., Oechel, W. C., Hyojung, K., Hongyan,
628 L., Wofsy, S. C., Dunn, A. L., Munger, J. W., Baldocchi, D. D., Liukang, X., Hollinger, D. Y.,
629 Richardson, A. D., Stoy, P. C., Siqueira, M. B. S., Monson, R. K., Burns, S. P., and Flanagan, L. B.:
630 Evaluation of remote sensing based terrestrial productivity from MODIS using regional tower eddy
631 flux network observations, IEEE T. Geosci. Remote, 44, 1908-1925, 10.1109/TGRS.2005.853936,
632 2006.
633 Hickler, T., Eklundh, L., Seaquist, J. W., Smith, B., Ardö, J., Olsson, L., Sykes, M. T., and
634 Sjöström, M.: Precipitation controls Sahel greening trend, Geophys. Res. Lett., 32, L21415,
635 doi:10.1029/2005GL024370, 2005.
636 Huber, S., Tagesson, T., and Fensholt, R.: An automated field spectrometer system for studying
637 VIS, NIR and SWIR anisotropy for semi-arid savanna, Remote Sens. Environ., 152, 547–556, 2014.
638 Huete, A., Didan, K., Miura, T., Rodriguez, E. P., Gao, X., and Ferreira, L. G.: Overview of the
639 radiometric and biophysical performance of the MODIS vegetation indices, Remote Sens. Environ.,
640 83, 195–213, 2002.
641 Ide, R., Nakaji, T., and Oguma, H.: Assessment of canopy photosynthetic capacity and estimation
642 of GPP by using spectral vegetation indices and the light-response function in a larch forest, Agric.
643 For. Meteorol., 150, 389-398, 2010.
644 Inoue, Y., Penuelas, J., Miyata, A., and Mano, M.: Normalized difference spectral indices for
645 estimating photosynthetic efficiency and capacity at a canopy scale derived from hyperspectral and
646 CO_2 flux measurements in rice, Remote Sens. Environ., 112, 156-172, 2008.
647 Jin, H., and Eklundh, L.: A physically based vegetation index for improved monitoring of plant
648 phenology, Remote Sens. Environ., 152, 512-525, http://dx.doi.org/10.1016/j.rse.2014.07.010, 2014.

649 Kanniah, K. D., Beringer, J., Hutley, L. B., Tapper, N. J., and Zhu, X.: Evaluation of Collections 4
650 and 5 of the MODIS Gross Primary Productivity product and algorithm improvement at a tropical
651 savanna site in northern Australia, Remote Sens. Environ., 113, 1808-1822,
652 http://dx.doi.org/10.1016/j.rse.2009.04.013, 2009.
653 Kanniah, K. D., Beringer, J., and Hutley, L. B.: The comparative role of key environmental factors
654 in determining savanna productivity and carbon fluxes: A review, with special reference to
655 Northern Australia, Progress in Physical Geography, 34, 459-490, 2010.
656 Kergoat, L., Lafont, S., Arneth, A., Le Dantec, V., and Saugier, B.: Nitrogen controls plant canopy
657 light-use efficiency in temperate and boreal ecosystems, J. Geophys. Res., 113, 1-19,
658 10.1029/2007JG000676, 2008.
659 Leblanc, M. J., Favreau, G., Massuel, S., Tweed, S. O., Loireau, M., and Cappelaere, B.: Land
660 clearance and hydrological change in the Sahel: SW Niger, Global Planet. Change, 61, 135-150,
661 http://dx.doi.org/10.1016/j.gloplacha.2007.08.011, 2008.
662 Levy, P. E., Moncrieff, J. B., Massheder, J. M., Jarvis, P. G., Scott, S. L., and Brouwer, J.: CO2
663 fluxes at leaf and canopy scale in millet, fallow and tiger bush vegetation at the HAPEX-Sahel
664 southern super-site, J. Hydrol., 188, 612-632, http://dx.doi.org/10.1016/S0022-1694(96)03195-2,
665 1997.
666 Ma, X., Huete, A., Yu, Q., Restrepo-Coupe, N., Beringer, J., Hutley, L. B., Kanniah, K. D.,
667 Cleverly, J., and Eamus, D.: Parameterization of an ecosystem light-use-efficiency model for
668 predicting savanna GPP using MODIS EVI, Remote Sens. Environ., 154, 253-271,
669 http://dx.doi.org/10.1016/j.rse.2014.08.025, 2014.
670 Mayaux, P., Bartholomé, E., Massart, M., Cutsem, C. V., Cabral, A., Nonguierma, A., Diallo, O.,
671 Pretorius, C., Thompson, M., Cherlet, M., Pekel, J.-F., Defourny, P., Vasconcelos, M., Gregorio, A.
672 D., S.Fritz, Grandi, G. D., C..Elvidge, P.Vogt, and Belward, A.: EUR 20665 EN –A Land-cover
673 map of Africa, edited by: Centre', E. C. J. R., European Commisions Joint Research Centre,
674 Luxembourg, 38 pp., 2003.
675 Mbow, C., Fensholt, R., Rasmussen, K., and Diop, D.: Can vegetation productivity be derived from
676 greenness in a semi-arid environment? Evidence from ground-based measurements, J. Arid
677 Environ., 97, 56-65, http://dx.doi.org/10.1016/j.jaridenv.2013.05.011, 2013.
678 Merbold, L., Ardö, J., Arneth, A., Scholes, R. J., Nouvellon, Y., de Grandcourt, A., Archibald, S.,
679 Bonnefond, J. M., Boulain, N., Brueggemann, N., Bruemmer, C., Cappelaere, B., Ceschia, E., El-
680 Khidir, H. A. M., El-Tahir, B. A., Falk, U., Lloyd, J., Kergoat, L., Le Dantec, V., Mougin, E.,
681 Muchinda, M., Mukelabai, M. M., Ramier, D., Roupsard, O., Timouk, F., Veenendaal, E. M., and
682 Kutsch, W. L.: Precipitation as driver of carbon fluxes in 11 African ecosystems, Biogeosciences, 6,
683 1027-1041, 10.5194/bg-6-1027-2009, 2009.
684 Moncrieff, J. B., Monteny, B., Verhoef, A., Friborg, T., Elbers, J., Kabat, P., de Bruin, H., Soegaard,
685 H., Jarvis, P. G., and Taupin, J. D.: Spatial and temporal variations in net carbon flux during
686 HAPEX-Sahel, J. Hydrol., 188–189, 563-588, 10.1016/s0022-1694(96)03193-9, 1997.
687 Monteith, J. L.: Solar radiation and productivity in tropical ecosystems, J. Appl. Ecol., 9, 747-766,
688 1972.
689 Monteith, J. L.: Climate and the efficiency of crop production in Britain, Philos. Trans. Roy. Soc. B.,
690 281, 277-294, 1977.
691 Monteny, B. A., Lhomme, J. P., Chehbouni, A., Troufleau, D., Amadou, M., Sicot, M., Verhoef, A.,
692 Galle, S., Said, F., and Lloyd, C. R.: The role of the Sahelian biosphere on the water and the CO2
693 cycle during the HAPEX-Sahel experiment, J. Hydrol., 188, 516-535,
694 http://dx.doi.org/10.1016/S0022-1694(96)03191-5, 1997.

Mutanga, O., and Skidmore, A. K.: Narrow band vegetation indices overcome the saturation problem in biomass estimation, Int. J. Remote Sens., 25, 3999-4014, 10.1080/01431160310001654923, 2004.
NASA: Reverb ECHO: http://reverb.echo.nasa.gov/reverb/, access: June 2016, 2016.
Papale, D., Reichstein, M., Aubinet, M., Canfora, E., Bernhofer, C., Kutsch, W., Longdoz, B., Rambal, S., Valentini, R., Vesala, T., and Yakir, D.: Towards a standardized processing of Net Ecosystem Exchange measured with eddy covariance technique: algorithms and uncertainty estimation, Biogeosciences, 3, 571-583, 10.5194/bg-3-571-2006, 2006.
Paruelo, J. M., Garbulsky, M. F., Guerschman, J. P., and Jobbágy, E. G.: Two decades of Normalized Difference Vegetation Index changes in South America: identifying the imprint of global change, Int. J. Remote Sens., 25, 2793-2806, 10.1080/01431160310001619526, 2004.
Poulter, B., Frank, D., Ciais, P., Myneni, R. B., Andela, N., Bi, J., Broquet, G., Canadell, J. G., Chevallier, F., Liu, Y. Y., Running, S. W., Sitch, S., and van der Werf, G. R.: Contribution of semi-arid ecosystems to interannual variability of the global carbon cycle, Nature, 509, 600-603, 10.1038/nature13376, 2014.
Prince, S. D., Kerr, Y. H., Goutorbe, J. P., Lebel, T., Tinga, A., Bessemoulin, P., Brouwer, J., Dolman, A. J., Engman, E. T., Gash, J. H. C., Hoepffner, M., Kabat, P., Monteny, B., Said, F., Sellers, P., and Wallace, J.: Geographical, biological and remote sensing aspects of the hydrologic atmospheric pilot experiment in the sahel (HAPEX-Sahel), Remote Sens. Environ., 51, 215-234, http://dx.doi.org/10.1016/0034-4257(94)00076-Y, 1995.
Qi, J., Chehbouni, A., Huete, A. R., Kerr, Y. H., and Sorooshian, S.: A modified soil adjusted vegetation index, Remote Sens. Environ., 48, 119-126, 1994.
Richter, K., Atzberger, C., Hank, T. B., and Mauser, W.: Derivation of biophysical variables from Earth observation data: validation and statistical measures, J. Appl. Remote Sens., 6, 063557, 10.1117/1.JRS.6.063557, 2012.
Rietkerk, M., Ketner, P., Stroosnijder, L., and Prins, H. H. T.: Sahelian rangeland development; a catastrophe?, J. Range Manage., 49, 512-519, 1996.
Rockström, J., and de Rouw, A.: Water, nutrients and slope position in on-farm pearl millet cultivation in the Sahel, Plant Soil, 195, 311-327, 10.1023/A:1004233303066, 1997.
Roujean, J.-L., and Breon, F.-M.: Estimating PAR absorbed by vegetation from bidirectional reflectance measurements, Remote Sens. Environ., 51, 375-384, http://dx.doi.org/10.1016/0034-4257(94)00114-3, 1995.
Rouse, J. W., Haas, R. H., Schell, J. A., Deering, D. W., and Harlan, J. C.: Monitoring the Vernal Advancement of Retrogradation of Natural Vegetation, Type III, Final Report, Greenbelt, MD, 1974.
Ruimy, A., Saugier, B., and Dedieu, G.: Methodology for the estimation of terrestrial net primary production from remotely sensed data., J. Geophys. Res., 99, 5263-5283., 1994.
Running, S. W., Nemani, R. R., Heinsch, F. A., Zhao, M., Reeves, M., and Hashimoto, H.: A Continuous Satellite-Derived Measure of Global Terrestrial Primary Production, BioScience, 54, 547-560, 10.1641/0006-3568(2004)054[0547:ACSMOG]2.0.CO;2, 2004.
Running, S. W., and Zhao, M.: User's Guide. Daily GPP and Annual NPP (MOD17A2/A3) Products NASA Earth Observing System MODIS Land Algorithm. Version 3.0 For Collection 6., University of Montana, USA, NASA, 2015.
Scholes, R. J., and Archer, S. R.: Tree-grass interactions in savannas, Annual Review of Ecology and Systematics, 28, 517-544, 1997.
Sellers, P. J., Dickinson, R. E., Randall, D. A., Betts, A. K., Hall, F. G., Berry, J. A., Collatz, G. J., Denning, A. S., Mooney, H. A., Nobre, C. A., Sato, N., Field, C. B., and Henderson-Sellers, A.:

Modeling the Exchanges of Energy, Water, and Carbon Between Continents and the Atmosphere, Science, 275, 502-509, 10.1126/science.275.5299.502, 1997.
Sims, D. A., Rahman, A. F., Cordova, V. D., El-Masri, B. Z., Baldocchi, D. D., Flanagan, L. B., Goldstein, A. H., Hollinger, D. Y., Misson, L., Monson, R. K., Oechel, W. C., Schmid, H. P., Wofsy, S. C., and Xu, L.: On the use of MODIS EVI to assess gross primary productivity of North American ecosystems, J. Geophys. Res., 111, G04015, 10.1029/2006JG000162, 2006.
Sjöström, M., Ardö, J., Eklundh, L., El-Tahir, B. A., El-Khidir, H. A. M., Hellström, M., Pilesjö, P., and Seaquist, J.: Evaluation of satellite based indices for gross primary production estimates in a sparse savanna in the Sudan, Biogeosciences, 6, 129-138, 2009.
Sjöström, M., Zhao, M., Archibald, S., Arneth, A., Cappelaere, B., Falk, U., de Grandcourt, A., Hanan, N., Kergoat, L., Kutsch, W., Merbold, L., Mougin, E., Nickless, A., Nouvellon, Y., Scholes, R. J., Veenendaal, E. M., and Ardö, J.: Evaluation of MODIS gross primary productivity for Africa using eddy covariance data, Remote Sens. Environ., 131, 275-286, http://dx.doi.org/10.1016/j.rse.2012.12.023, 2013.
Tagesson, T., Eklundh, L., and Lindroth, A.: Applicability of leaf area index products for boreal regions of Sweden, Int. J. Remote Sens., 30, 5619–5632, 2009.
Tagesson, T., Fensholt, R., Cropley, F., Guiro, I., Horion, S., Ehammer, A., and Ardö, J.: Dynamics in carbon exchange fluxes for a grazed semi-arid savanna ecosystem in West Africa, Agr. Ecosyst. Environ., 205, 15-24, http://dx.doi.org/10.1016/j.agee.2015.02.017, 2015a.
Tagesson, T., Fensholt, R., Guiro, I., Rasmussen, M. O., Huber, S., Mbow, C., Garcia, M., Horion, S., Sandholt, I., Rasmussen, B. H., Göttsche, F. M., Ridler, M.-E., Olén, N., Olsen, J. L., Ehammer, A., Madsen, M., Olesen, F. S., and Ardö, J.: Ecosystem properties of semi-arid savanna grassland in West Africa and its relationship to environmental variability, Global Change Biol., 21, 250-264, doi: 10.1111/gcb.12734, 2015b.
Tagesson, T., Fensholt, R., Huber, S., Horion, S., Guiro, I., Ehammer, A., and Ardö, J.: Deriving seasonal dynamics in ecosystem properties of semi-arid savannas using in situ based hyperspectral reflectance, Biogeosciences, 12, 4621-4635, doi:10.5194/bg-12-4621-2015, 2015c.
Tagesson, T., Fensholt, R., Cappelaere, B., E., M., Horion, S., L., K., Nieto, H., Ehammer, A., Demarty, J., and Ardö, J.: Spatiotemporal variability in carbon exchange fluxes across the Sahel Agric. For. Meteorol., 226–227, 108-118, 2016a.
Tagesson, T., Fensholt, R., Guiro, I., Cropley, F., Horion, S., Ehammer, A., and Ardö, J.: Very high carbon exchange fluxes for a grazed semi-arid savanna ecosystem in West Africa, Danish Journal of Geography, 116, 93-109, http://dx.doi.org/10.1080/00167223.2016.1178072 2016b.
Timouk, F., Kergoat, L., Mougin, E., Lloyd, C. R., Ceschia, E., Cohard, J. M., Rosnay, P. d., Hiernaux, P., Demarez, V., and Taylor, C. M.: Response of surface energy balance to water regime and vegetation development in a Sahelian landscape, J. Hydrol., 375, 12-12, 10.1016/j.jhydrol.2009.04.022, 2009.
Turner, D. P., Ritts, W. D., Cohen, W. B., Maeirsperger, T. K., Gower, S. T., Kirschbaum, A. A., Running, S. W., Zhao, M., Wofsy, S. C., Dunn, A. L., Law, B. E., Campbell, J. L., Oechel, W. C., Kwon, H. J., Meyers, T. P., Small, E. E., Kurc, S. A., and Gamon, J. A.: Site-level evaluation of satellite-based global terrestrial gross primary production and net primary production monitoring, Global Change Biol., 11, 666-684, 2005.
Turner, D. P., Ritts, W. D., and Cohen, W. B.: Evaluation of MODIS NPP and GPP products across multiple biomes, Remote Sens. Environ., 102, 282-293, 2006.
United Nations: Sahel Regional Strategy Mid-Year Review 2013 New York, 1-59, 2013.
Veenendaal, E. M., Kolle, O., and Lloyd, J.: Seasonal variation in energy fluxes and carbon dioxide exchange for a broadleaved semi-arid savanna (Mopane woodland) in Southern Africa, Global Change Biol., 10, 318-328, 2004.

790 Velluet, C., Demarty, J., Cappelaere, B., Braud, I., Issoufou, H. B. A., Boulain, N., Ramier, D.,
791 Mainassara, I., Charvet, G., Boucher, M., Chazarin, J. P., Oï, M., Yahou, H., Maidaji, B., Arpin-
792 Pont, F., Benarrosh, N., Mahamane, A., Nazoumou, Y., Favreau, G., and Seghieri, J.: Building a
793 field- and model-based climatology of local water and energy cycles in the cultivated Sahel; annual
794 budgets and seasonality, Hydrol. Earth Syst. Sci., 18, 5001-5024, 10.5194/hess-18-5001-2014, 2014.
795 Yoder, B. J., and Pettigrew-Crosby, R. E.: Predicting nitrogen and chlorophyll content and
796 concentrations from reflectance spectra (400–2500 nm) at leaf and canopy scales, Remote Sens.
797 Environ., 53, 199-211, http://dx.doi.org/10.1016/0034-4257(95)00135-N, 1995.
798 Zhang, Y., Guanter, L., Berry, J. A., Joiner, J., van der Tol, C., Huete, A., Gitelson, A., Voigt, M.,
799 and Köhler, P.: Estimation of vegetation photosynthetic capacity from space-based measurements
800 of chlorophyll fluorescence for terrestrial biosphere models, Global Change Biol., 20, 3727-3742,
801 10.1111/gcb.12664, 2014.

802

803

Tables

Table 1. Description of the six measurement sites including location, soil type, ecosystem type and dominant species.

Measurement site	Coordinates	Soil type	Ecosystem	Dominant species
Agoufou[a] (ML-AgG, Mali)	15.34°N, 1.48°W	Sandy ferruginous Arenosol	Open woody savannah (4% tree cover)	Trees: *Acacia spp.*, *Balanites aegyptiaca*, *Combretum glutinosum* Herbs: *Zornia glochidiata*, *Cenchrus biflorus*, *Aristida mutabilis*, *Tragus berteronianus*
Dahra[b] (SN-Dah, Senegal)	15.40°N, 15.43°W	Sandy luvic arenosol	Grassland/shrubland Savanna (3% tree cover)	Trees: *Acacia spp.*, *Balanites aegyptiaca* Herbs: *Zornia latifolia*, *Aristida adscensionis*, *Cenchrus biflorus*
Demokeya[c] (SD-Dem, Sudan)	13.28°N, 30.48°E	Cambic Arenosol	Sparse acacia savannah (7% tree cover)	*Trees: Acacia spp.*, Herbs: *Aristida pallida*, *Eragrostis tremula*, *Cenchrus biflorus*
Kelma[a] (ML-Kem, Mali)	15.22°N, 1.57°W	Clay soil depression	Open acacia forest (90% tree cover)	Trees: *Acacia seyal*, *Acacia nilotica*, *Balanites aegyptiaca* Herbs: *Sporobolus hevolvus*, *Echinochloa colona*, *Aeschinomene sensitive*
Wankama Fallow[d] (NE-WaF, Niger)	13.65°N, 2.63°E	Sandy ferruginous Arenosol	Fallow bush	*Guiera senegalensis*
Wankama Millet[e] (NE-WaM, Niger)	13.64°N, 2.63°E	Sandy ferruginous Arenosol	Millet crop	*Pennisetum glaucum*

[a](Timouk et al., 2009)
[b](Tagesson et al., 2015b)
[c](Sjöström et al., 2009)
[d](Velluet et al., 2014)
[e](Boulain et al., 2009)

Table 2. Correlation between intra-annual dynamics in photosynthetic capacity (F_{opt}; F_{opt_frac} for all sites), quantum efficiency (α; α_{frac} for all sites), and the different vegetation indices for the six measurement sites (Fig. 1). Values are averages±1 standard deviation from 200 bootstraping runs. The bold values are the indices with the strongest correlation. EVI is the enhanced vegetation index, NDVI is the normalized difference vegetation index, RDVI is the renormalized difference vegetation index, SIWSI is the shortwave infrared water stress index. $SIWSI_{12}$ is based on the MODIS Bidirectional Reflectance Distribution Functions (NBAR) band 2 and band 5, whereas $SIWSI_{16}$ is based on MODIS NBAR band 2 and band 6.

Measurement site	F_{opt}					α				
	EVI	NDVI	RDVI	$SIWSI_{12}$	$SIWSI_{16}$	EVI	NDVI	RDVI	$SIWSI_{12}$	$SIWSI_{16}$
ML-AgG	0.89±0.02	0.87±0.02	0.95±0.01	**-0.95±0.01**	-0.93±0.02	0.92±0.02	0.91±0.01	**0.96±0.01**	-0.94±0.01	-0.88±0.02
SN-Dah	0.92±0.005	0.91±0.01	0.96±0.003	**-0.96±0.004**	-0.93±0.01	0.89±0.01	0.90±0.01	**0.93±0.01**	-0.92±0.01	-0.87±0.01
SD-Dem	0.81±0.01	0.78±0.01	0.91±0.01	**-0.93±0.01**	-0.90±0.01	0.76±0.02	0.73±0.02	**0.86±0.01**	-0.82±0.02	-0.79±0.02
MA-Kem	0.77±0.02	0.83±0.02	0.95±0.01	**-0.95±0.01**	-0.90±0.02	0.69±0.05	0.73±0.04	**0.80±0.03**	-0.77±0.03	-0.76±0.03
NE-WaF	0.87±0.02	0.81±0.02	0.78±0.02	**-0.90±0.01**	-0.80±0.02	**0.89±0.01**	0.84±0.01	0.85±0.01	-0.88±0.01	-0.79±0.01
NE-WaM	0.41±0.05	0.50±0.04	**0.72±0.03**	-0.55±0.04	-0.43±0.05	0.72±0.02	0.76±0.02	**0.81±0.01**	-0.75±0.01	-0.72±0.01
All sites	0.86±0.0	0.79±0.0	**0.90±0.0**	0.75±0.0	0.70±0.0	0.83±0.01	0.80±0.01	**0.86±0.01**	0.62±0.01	0.54±0.01

Table 3. Statistics for the regression tree analysis. The regression tree analysis was used for studying relationships between intra-annual dynamics in the the photosynthetic capacity (F_{opt}; F_{opt_frac} for all sites) and quantum efficiency (α; $\alpha_{\_frac}$ for all sites) and the explanatory variables for the six measurement sites (Fig. 1). The pruning level is the number of splits of the regression tree and an indication of complexity of the system.

Measurement site	Explanatory variables:					Pruning level	R^2
F_{opt}	1	2	3	4	5		
ML-AgG	$SIWSI_{12}$	Tair	PAR	SWC		16	0.98
SN-Dah	$SIWSI_{12}$	SWC	VPD	Tair	PAR	84	0.98
SD-Dem	$SIWSI_{12}$	VPD	SWC	Tair	PAR	33	0.97
ML-Kem	$SIWSI_{12}$	PAR	Tair	VPD		22	0.98
NE-WaF	$SIWSI_{12}$	SWC	VPD	Tair		14	0.92
NE-WaM	RDVI	SWC	VPD	Tair		18	0.75
All sites	RDVI	SWC	Tair	VPD		16	0.87
α							
ML-AgG	RDVI					3	0.95
SN-Dah	RDVI	VPD	SWC	Tair	PAR	21	0.93
SD-Dem	RDVI	SWC	PAR	Tair		16	0.93
ML-Kem	RDVI	Tair				4	0.75
NE-WaF	EVI	SWC	VPD			10	0.90
NE-WaM	RDVI	SWC	VPD	Tair		15	0.86
All sites	RDVI	SWC	VPD	Tair		16	0.84

Table 4. Annual peak values of quantum efficiency (α_{peak}; μmol CO_2 μmol PAR^{-1}) and photosynthetic capacity (F_{opt_peak}; μmol CO_2 m^{-2} s^{-1}) for the six measurement sites (Fig. 1). The peak values are the 2 week running mean with highest annual value.

Measurement site	Year	α_{peak}	F_{opt_peak}
ML-AgG	2007	0.0396	24.5
SN-Dah	2010	0.0638	50.0
	2011	0.0507	42.3
	2012	0.0480	39.2
	2013	0.0549	40.0
SD-Dem	2007	0.0257	16.5
	2008	0.0327	21.0
	2009	0.0368	16.5
ML-Kem	2007	0.0526	33.5
NE-WaF	2005	0.0273	18.2
	2006	0.0413	21.0
NE-WaM	2005	0.0252	10.6
	2006	0.0200	10.1
Average		0.0399	26.4

Table 5. Correlation matrix between annual peak values of photosynthetic capacity (F_{opt_peak}) and quantum efficiency (α_{peak}) and measured environmental variables. P is annual rainfall; T_{air} is yearly averaged air temperature at 2 m height; SWC is yearly averaged soil water content (% volumetric water content) measured at 0.1 m depth; Rh is yearly averaged relative humidity; VPD is yearly averaged vapour pressure deficit; R_g is yearly averaged incoming global radiation; N and C cont. are soil nitrogen and carbon contents; $NDVI_{peak}$ is annual peak normalized difference vegetation index (NDVI); EVI_{peak} is annual peak enhanced vegetation index (EVI); $RDVI_{peak}$ is annual peak renormalized difference vegetation index (RDVI); $SIWSI_{12peak}$ is annual peak short wave infrared water stress index based on MODIS NBAR band 2 and band 5; and $SIWSI_{16peak}$ is annual peak short wave infrared water stress index based on MODIS NBAR band 2 and band 6. Sample size was 13 for all except the marked explanatory variables.

Explanatory variable	F_{opt_peak}	α_{peak}
Meteorological data		
P (mm)	0.24±0.26	0.13±0.27
T_{air} (°C)	-0.07±0.25	-0.01±0.25
SWC (%)[a]	0.33±0.25	0.16±0.27
Rh (%)	0.73±0.16*	0.60±0.19
VPD (hPa)	0.20±0.26	0.15±0.30
R_g (W m^{-2})	-0.48±0.21	-0.41±0.24
Biomass and edaphic data		
Biomass (g DW m^{-2})[a]	0.77±0.15*	0.74±0.14*
C3/C4 ratio	-0.05±0.26	0.06±0.30
N cont. (%)[b]	0.22±0.11	0.35±0.14
C cont. (%)[b]	0.89±0.06**	0.87±0.07**
Earth observation data		
$NDVI_{peak}$	0.94±0.05**	0.87±0.07**
EVI_{peak}	0.93±0.04**	0.87±0.07**
$RDVI_{peak}$	0.93±0.04**	0.89±0.07**
$SIWSI_{12peak}$	0.85±0.08**	0.84±0.08**
$SIWSI_{16peak}$	0.67±0.12*	0.65±0.15*
Photosynthetic variables		
F_{opt}	-	0.94±0.03**

[a]sample size equals 11.
[b]sample size equals 9.
* significant at 0.05 level.
** significant at 0.01 level

Table 6. Statistics regarding the evaluation of the gross primary ~~productivity~~production (GPP) model for the six measurement sites (Fig. 1). In situ and modelled GPP are averages ± 1 standard deviation. RMSE is the root-mean-squares-error, and slope, intercept and R^2 is from the fitted ordinary least squares linear regression.

Measurement site	In situ GPP (µmol CO_2 m^{-2} s^{-1})	Modelled GPP (µmol CO_2 m^{-2} s^{-1})	RMSE (µmol CO_2 m^{-2} s^{-1})	slope	Intercept (µmol CO_2 m^{-2} s^{-1})	R^2
ML-AgG	5.353.55±5.456.38	53.9791±5.5480	1.832.48±0.10	0.9784±0.06003	0.501.46±0.0301	0.9086±0.0021
SN-Dah	9.1439±10.1217	8.6087±10.729.67	3.8599±1.34	0.9988±0.07002	-0.440.62±1.110.01	0.8785±0.04001
SD-Dem	3.834.26±4.4255	3.6198±4.513.90	3.0515±1.06	0.7963±0.18003	0.611.31±0.75.007	0.5954±0.1102
ML-Kem	11.1716±7.988.02	10.7352±10.509.22	5.064.35±1.23	1.1602±0.20003	-2.29-0.82±1.650.03	0.7978±0.12002
NE-WaF	3.915.77±4.0817	5.386.63±3.5973	2.5547±1.05	0.8570±0.15005	2.0858±1.480.02	0.7569±0.08003
NE-WaM	2.253.04±2.001.93	5.516.35±3.9347	4.1312±0.99	1.6331±0.45004	1.842.37±1.010.02	0.6853±0.035
Average	5.316.73±7.1572	5.807.02±7.5339	3.5668±0.6055	0.9483±0.07	0.851.34±0.9282	0.84±0.0807

Table 7. The parameters for Eq. ~~18~~ 13 that was used in the final gross primary ~~productivity~~production (GPP) model. RMSE is the root mean square error, and R^2 is the coefficient of determination ~~of~~ for the ~~linear~~ regression models predicting the different variables.

Parameter	Value	RMSE	R^2
k_{Fopt}	79.6±6.3	5.1±1.3	0.89±0.05
m_{Fopt}	-7.3±3.2		
l_{Fopt}	~~1.81~~3.51±0.~~07~~19	0.~~33~~15±0.~~04~~02	0.~~79~~88±0.0~~6~~4
n_{Fopt}	~~0.85~~0.03±0.~~07~~006		
~~k_α~~	0.16±0.02	0.0069±0.0021	0.81±0.10
m_α	-0.014±0.007		
l_α	~~1.20~~3.75±0.~~05~~27	0.~~38~~20±0.~~04~~02	0.~~71~~80±0.~~04~~10
n_α	~~-0.98~~0.02±0.0~~6~~7		

Figures

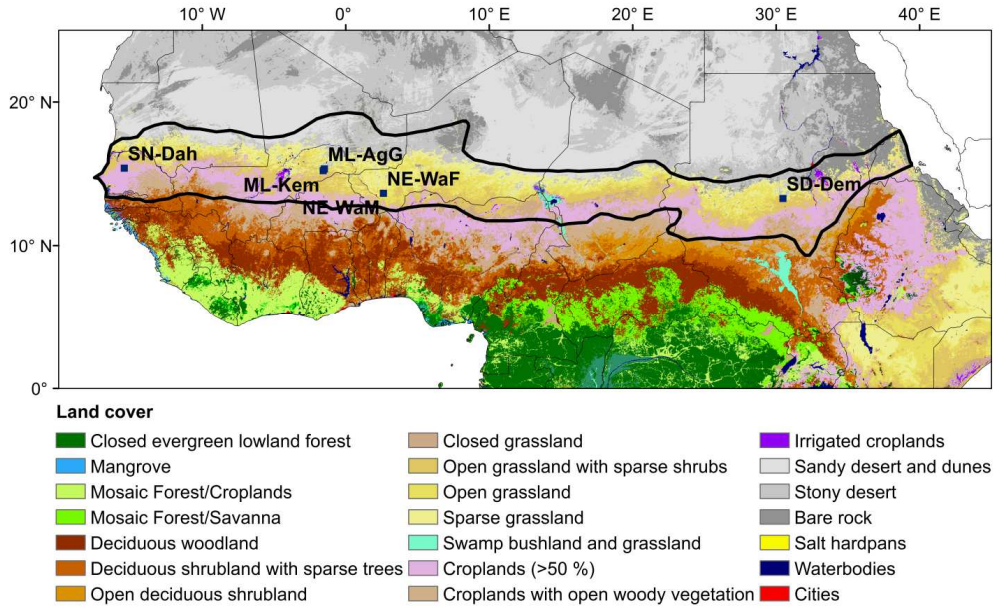

Figure 1. Land ~~use~~ cover classes for the Sahel and the location of the six measurement sites included in the study. The land cover classes are based on multi-sensor satellite observations (Mayaux et al., 2003). The sites are Agoufou (ML-AgG), Dahra (SN-Dah), Demokeya (SD-Dem), Kelma (ML-Kem), Wankama Fallow (NE-WaF), and Wankama Millet (NE-WaM). The thick black line is the borders of the Sahel based on the isohytes 150 and 700 mm of annual precipitation (Prince et al., 1995).

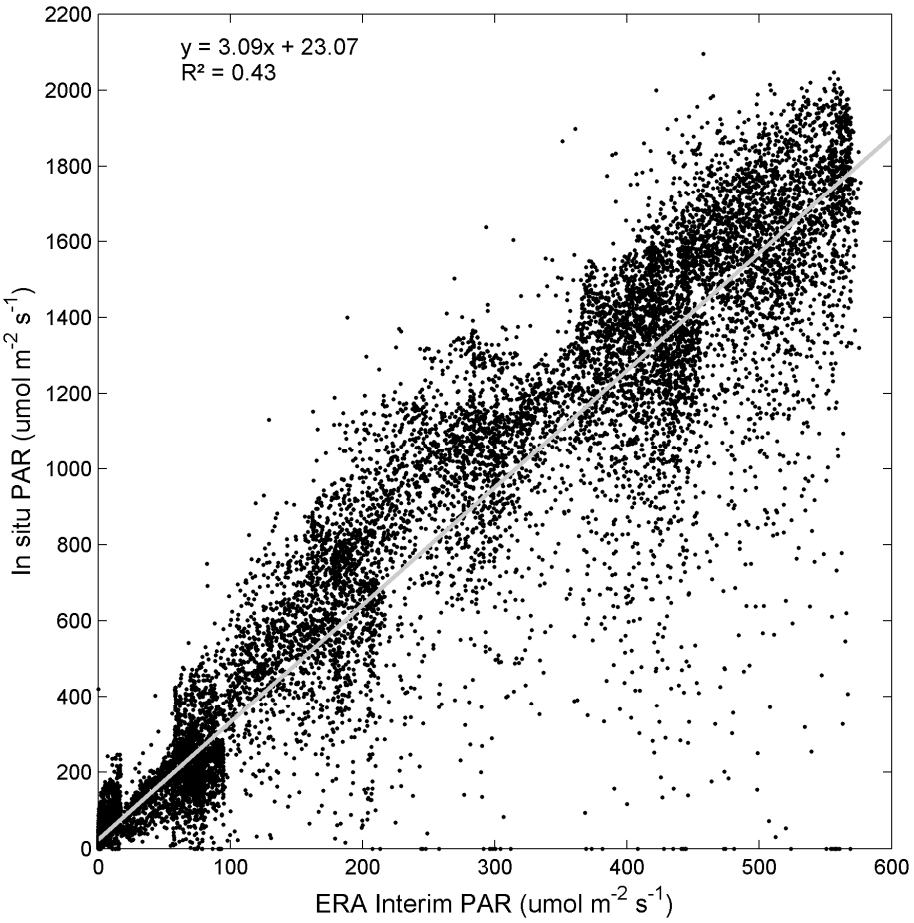

Figure 2. Photosynthetically active radiation (PAR) measured in situ against gridded ERA Interim ground surface PAR extracted for the six measurement sites (Figure 1) across the Sahel from European Centre for Medium-Range Weather Forecasts, ECMWF (2016b). The grey line is the ordinary least square linear regression.

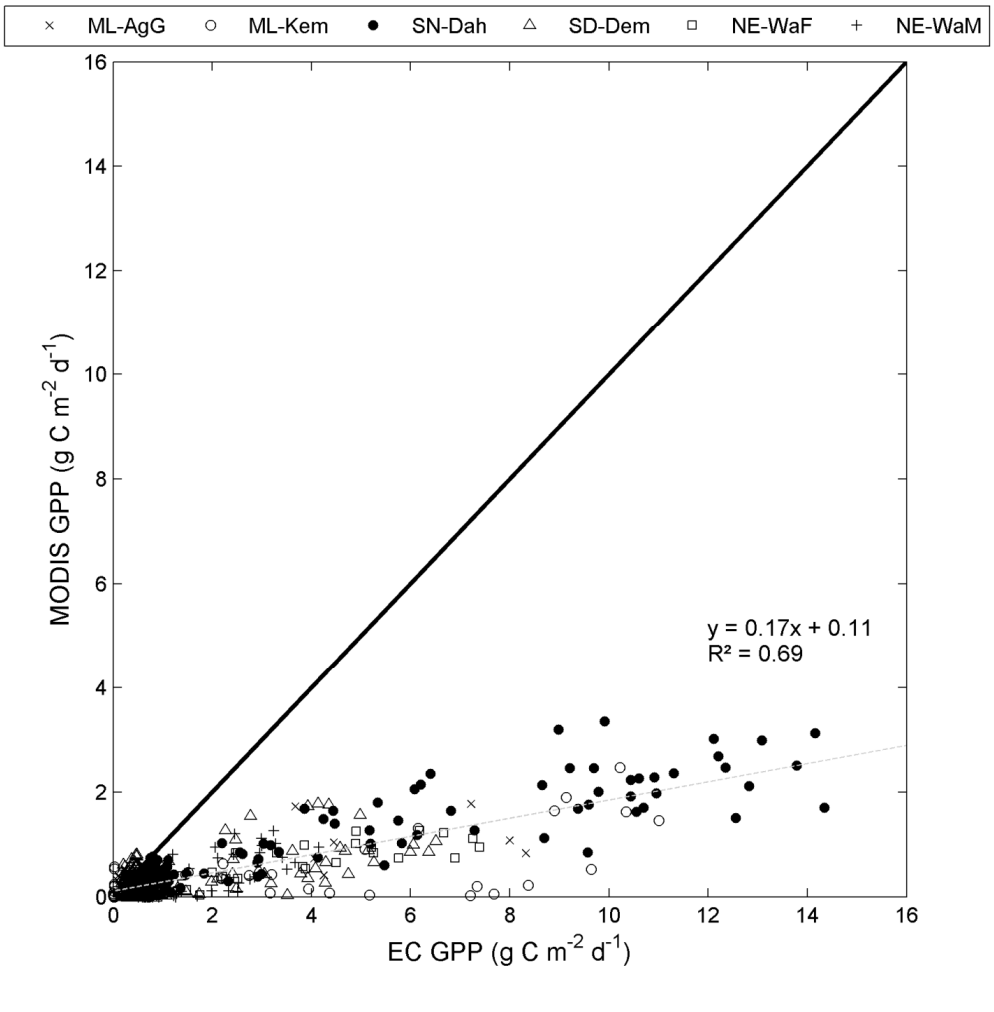
ML-AgG
ML-Kem
SN-Dah
SD-Dem
NE-WaF
NE-WaM
MODIS GPP (g C m-2 d-1)
EC GPP (g C m-2 d-1)
y = 0.17x + 0.11
R² = 0.69
0
2
4
6
8
10
12
14
16

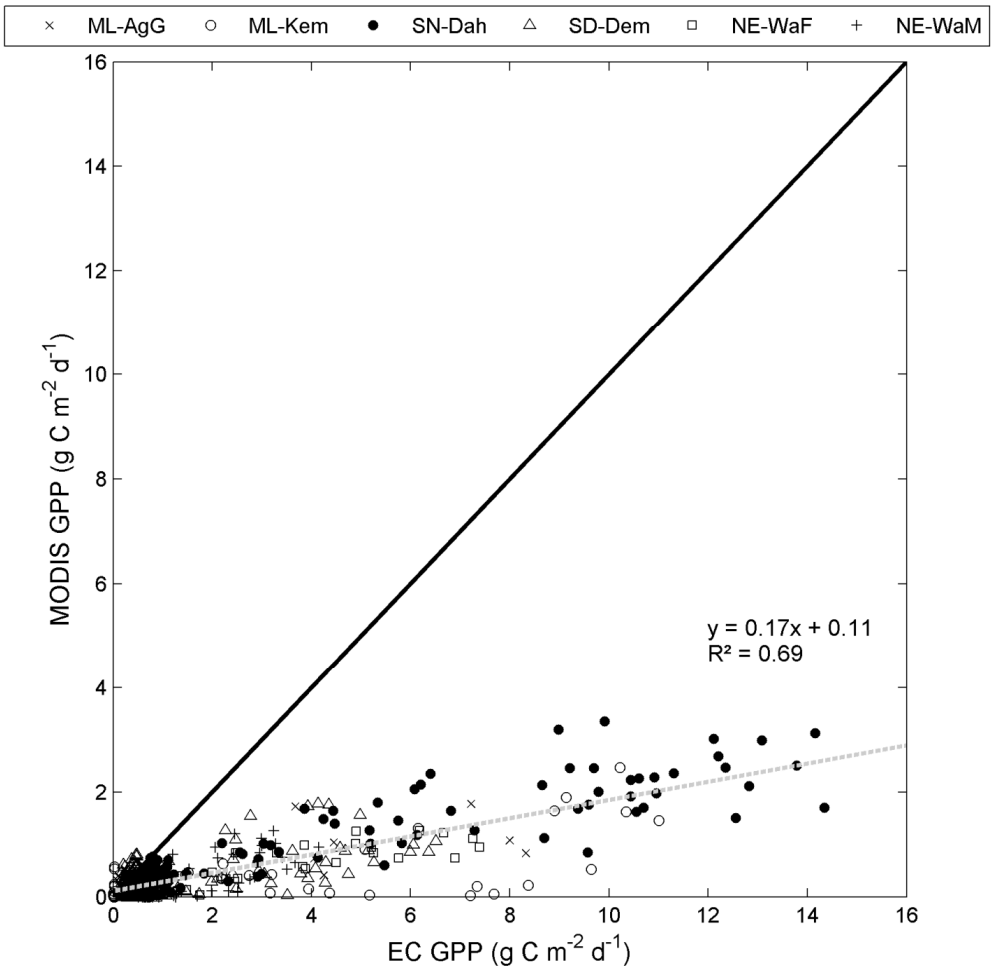

Figure ~~3~~2. Evaluation of the MODIS based GPP product MOD17A2H collection 6 against eddy covariance based GPP from the six measurement sites (Fig. 1) across the Sahel. The thick black line shows the one-to-one ratio, and the ~~thin~~ grey dotted line is the fitted ordinary least square linear regression.

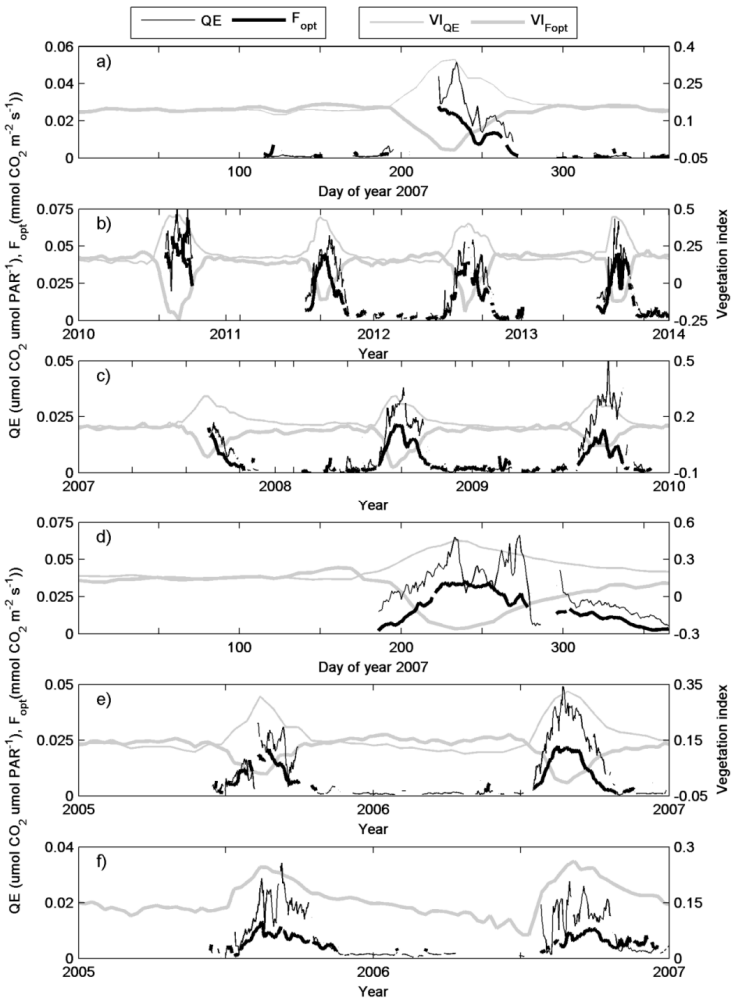
QE
F_{opt}
VI_{QE}
VI_{Fopt}
a)
b)
c)
d)
e)
f)
QE (umol CO_2 umol PAR^{-1}), F_{opt}(mmol CO_2 m^{-2} s^{-1}))
Vegetation index
Day of year 2007
Year

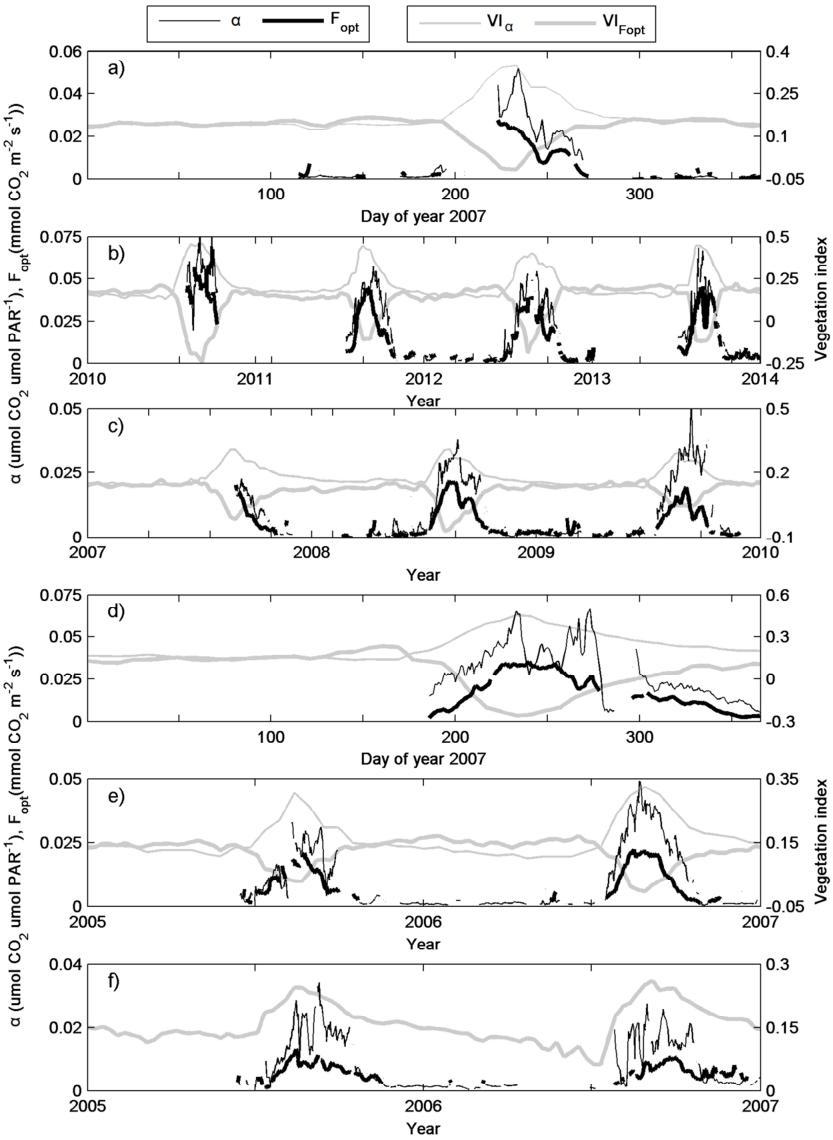
α
F opt
VI α
VI Fopt
a)
b)
c)
d)
e)
f)
α (umol CO2 umol PAR-1), F opt(mmol CO2 m-2 s-1))
Vegetation index
Day of year 2007
Year

Figure 43. Dynamics in photosynthetic capacity (F_{opt}) and quantum efficiency (~~QE,~~ α) for the six measurement sites. Included is also dynamics in the vegetation indices with highest correlation to the intra-annual dynamics in F_{opt} (VI_{Fopt}) and to quantum efficiency (VI_{α}~~$_{QE}$~~) (Table 2). The sites are a) Agoufou (ML-AgG), b) Dahra (SN-Dah), c) Demokeya (SD-Dem), d) Kelma (ML-Kem), e) Wankama Fallow (NE-WaF), and f) Wankama Millet (NE-WaM).

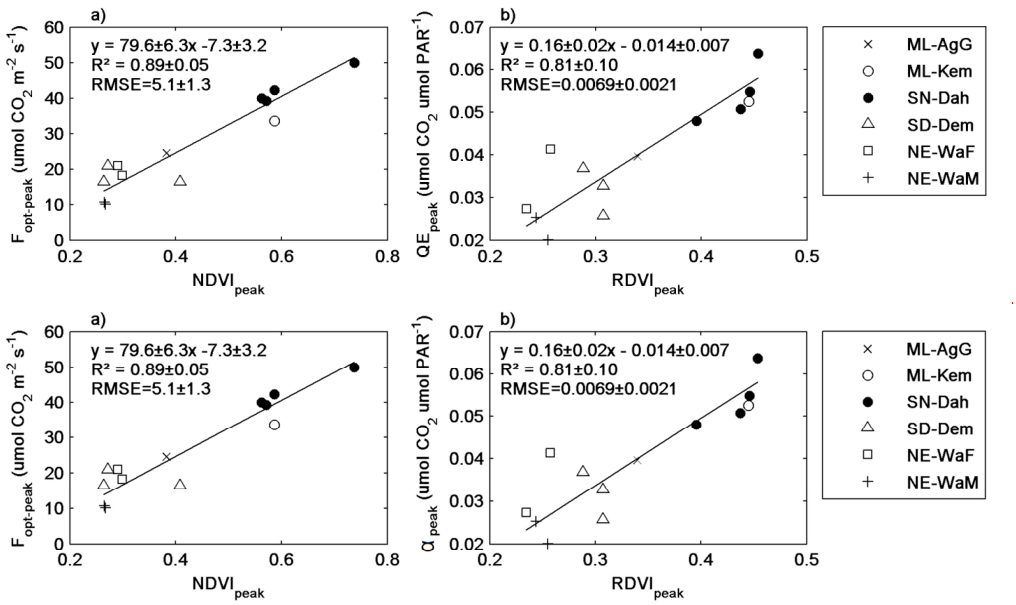

Figure ~~5~~4. Scatter plots of annual peak values for the six measurement sites (Fig. 1) of a) photosynthetic capacity (F_{opt_peak}) and b) quantum efficiency (~~$QE_{peak;}$~~ α_{peak}) against peak values of normalized difference vegetation index ($NDVI_{peak}$) and renormalized difference vegetation index ($RDVI_{peak}$), respectively. The annual peak values were estimated by taking the annual maximum of a two week running mean.

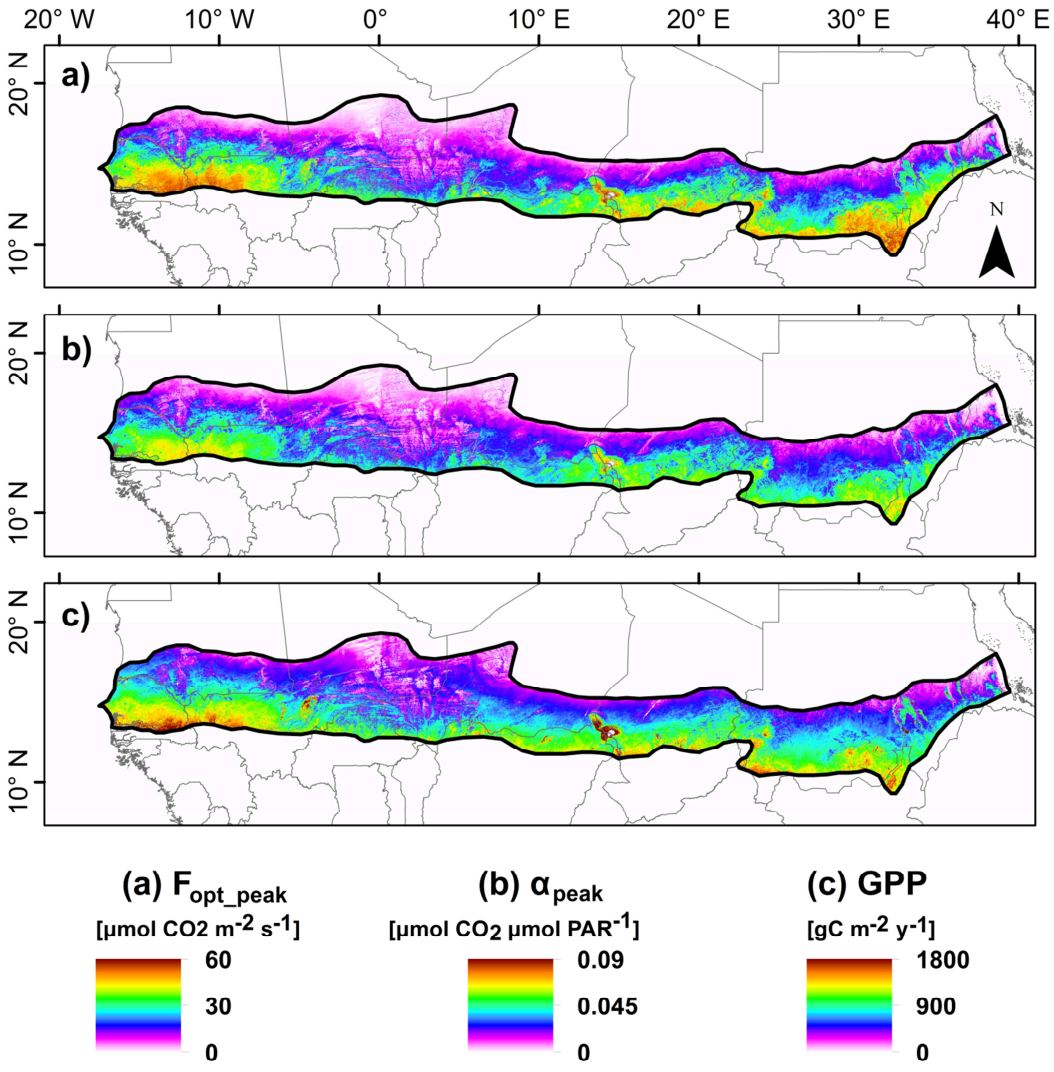

Figure 5. Maps of a) peak values of photosynthetic capacity (F_{opt_peak}) averaged for 2001-2014, b) peak values of quantum efficiency (α_{peak}) averaged for 2001-2014, and c) annual budgets of GPP averaged for 2001-2014.

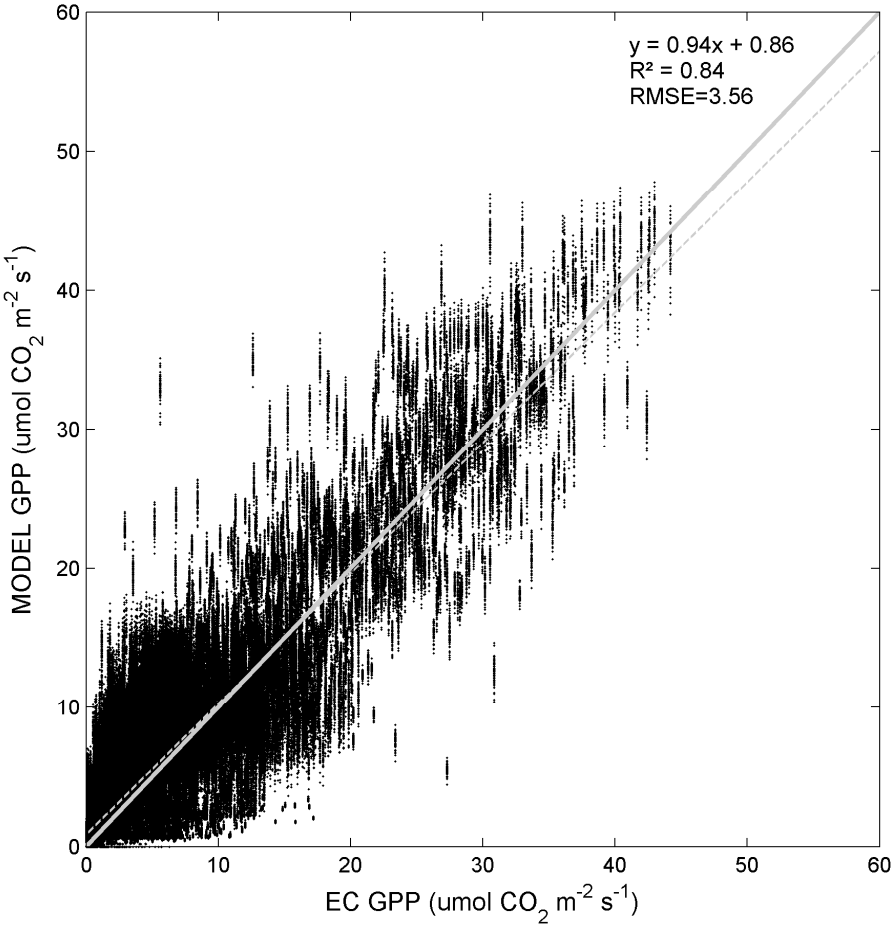
y = 0.94x + 0.86
R² = 0.84
RMSE=3.56
MODEL GPP (umol CO2 m-2 s-1)
EC GPP (umol CO2 m-2 s-1)
0
10
20
30
40
50
60

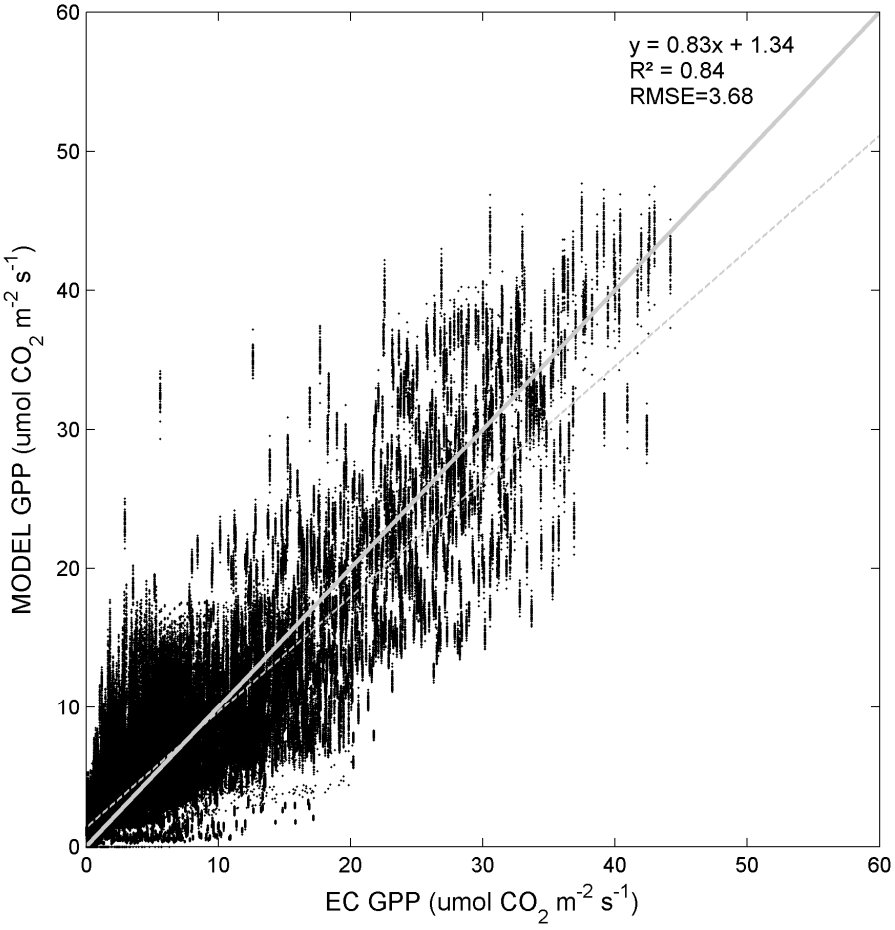

Figure 6. Evaluation of the modelled gross primary ~~productivity~~production (GPP) (Eq. ~~18~~13) against in situ GPP from all six measurement sites across the Sahel. The thick grey line shows the one-to-one ratio, whereas the dotted thin grey line is the fitted ordinary least square linear regression.

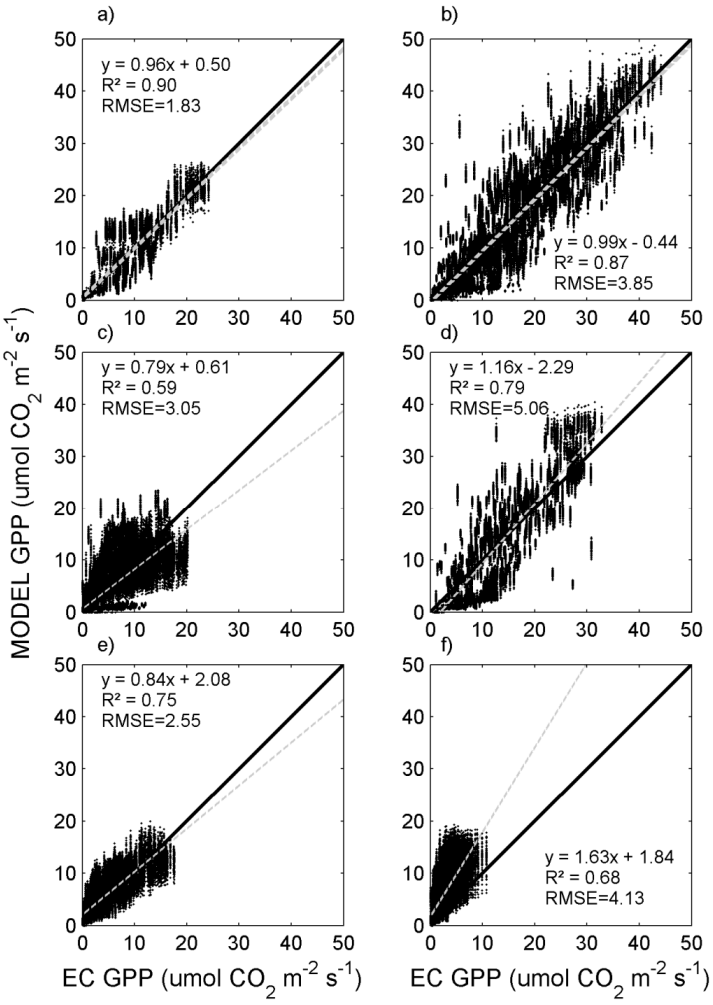
a)
y = 0.96x + 0.50
R² = 0.90
RMSE=1.83
b)
y = 0.99x - 0.44
R² = 0.87
RMSE=3.85
c)
y = 0.79x + 0.61
R² = 0.59
RMSE=3.05
d)
y = 1.16x - 2.29
R² = 0.79
RMSE=5.06
e)
y = 0.84x + 2.08
R² = 0.75
RMSE=2.55
f)
y = 1.63x + 1.84
R² = 0.68
RMSE=4.13
MODEL GPP (umol CO2 m-2 s-1)
EC GPP (umol CO2 m-2 s-1)
EC GPP (umol CO2 m-2 s-1)

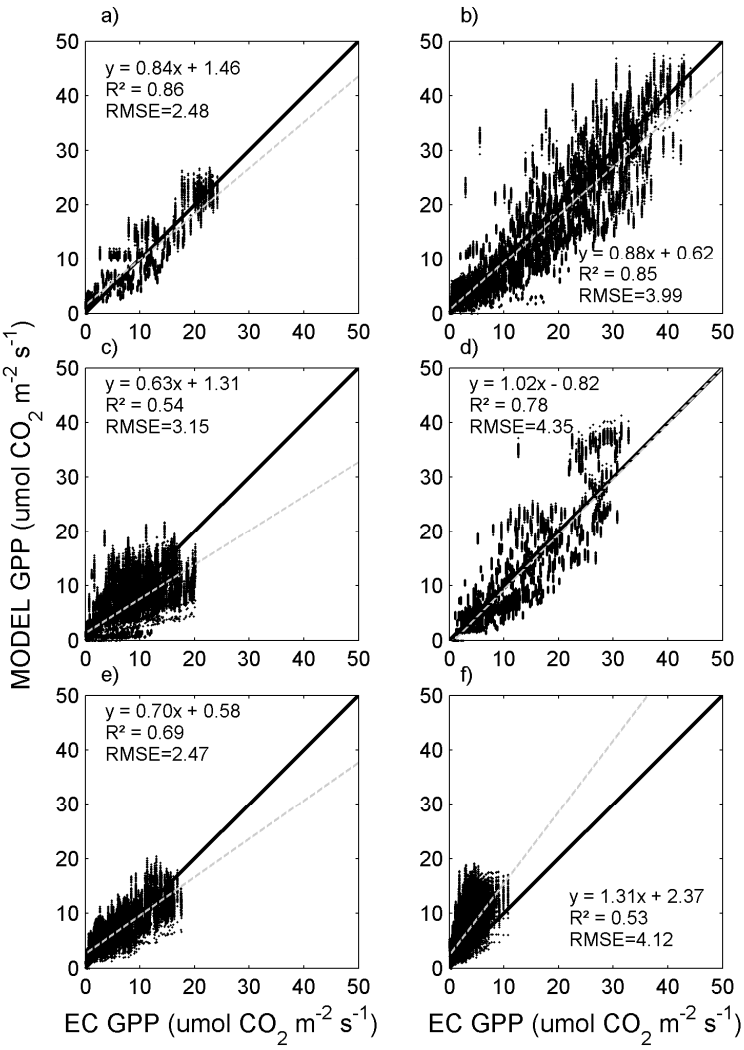

Figure 7. Evaluation of the modelled gross primary ~~productivity~~production (GPP) (Eq. ~~18~~13) against in situ GPP for the six sites across Sahel (Fig. 1). The thick black line shows the one-to-one ratio, whereas the dotted thin grey line is the fitted

ordinary least square linear regression. The sites are a) Agoufou (ML-AgG), b) Dahra (SN-Dah), c) Demokeya (SD-Dem), d) Kelma (ML-Kem), e) Wankama Fallow (NE-WaF), and f) Wankama Millet (NE-WaM).